

Development of Polyimide/Metal  
Gradient Microcomposite Films

by

Leslie Sauder Horning

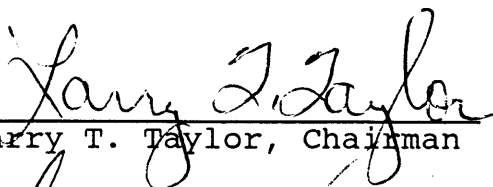
Thesis submitted to the Faculty of the  
Virginia Polytechnic Institute and State University  
in partial fulfillment of the requirements for the degree of

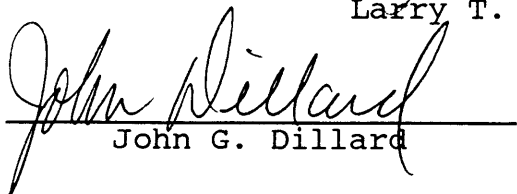
Master of Science

in

Chemistry

APPROVED:

  
Larry T. Taylor, Chairman

  
John G. Dillard

  
James P. Wightman

January, 1990

Blacksburg, Virginia

**Development of Polyimide/Metal  
Gradient Microcomposite Films**

by

Leslie Sauder Horning

Larry T. Taylor: Chairman

Chemistry

(ABSTRACT)

Polyimides are attractive polymers because of valued intrinsic properties such as high thermal stability and good solvent resistance. At the same time, much effort is put into modifying polyimides to introduce different properties. This thesis describes a study where polyimides were modified with soluble metal compounds in an effort to create microcomposite films in which the location of the composite structure was controlled; namely at the film interfaces. Two different modification techniques were used in this study, in-situ chemical generation and infusion deposition. Results indicate that infusion deposition was successful in producing a gradient microcomposite structure in polyimide films when silver(I)nitrate was the metal dopant. Analysis revealed that formation of the microcomposite structure depends upon the glass transition temperature and precure temperature of the polyimide film being modified.

## DEDICATION

To my God,  
who gave me my intellect;

To my parents, Reuben and Sarah Horning,  
who always gave me encouragement;

To my extraordinary wife, Crystal,  
who showed me love and support by  
moving to Blacksburg with me, even at  
the sake of her own career.

## ACKNOWLEDGEMENTS

This thesis is a culmination of a long journey which would not have been possible without the help and encouragement of a variety of persons along the way.

First of all, I would like to express deep appreciation and admiration for my high school chemistry teacher, Wilmer Nolt, who, through his words and example, instilled in me a fascination and an interest in the wide world of chemistry.

To one of my undergraduate professors, Dr. Gary Stucky, I am grateful for having the contacts in place to help make available to me the opportunity to experience chemistry research first-hand at Virginia Tech while an undergraduate.

I want to thank my advisor, Dr. Larry Taylor, for his probing questions, challenging of results, encouragement and moral support, all in the effort to help me reach my full potential in the field of chemistry. I also appreciate the advice and technical contributions of my other committee members, Dr. John Dillard and Dr. James Wightman, particularly in the early part of this thesis.

Dr. James Rancourt deserves special thanks as one who had an answer to every question; his contributions were invaluable, including Figures 1 and 2.

I would like to thank Michelle Porta for an excellent job in obtaining the TEM data for me. Thanks also go to Jim

Hollenhead and Frank Cromer for help in obtaining and interpreting the XPS data. I deeply appreciate the lab work of Matt Ellison, a summer undergraduate research assistant from Wollford College, who did much of the sample preparation for the infusion deposition study.

I want to thank Greg Porta, Suren Rodrigues and Bill Murray for their support, encouragement and constructive criticisms during group meetings.

Finally, I would like to express deep appreciation to Dr. Karl Wefers and Alcoa Technical Center for providing materials and the financial and technical input which made this study possible in the first place.

## Table of Contents

|  |            |
|--|------------|
| <b>List of Structures.....</b>                       | <b>ix</b>  |
| <b>List of Illustrations.....</b>                    | <b>x</b>   |
| <b>List of Tables.....</b>                           | <b>xii</b> |
| <br>   |            |
| <b>I. Introduction.....</b>                          | <b>1</b>   |
| <br>   |            |
| <b>II. Literature Review.....</b>                    | <b>7</b>   |
| A. Introduction.....                                 | 7          |
| B. Preparation of Polymeric Composite Materials..... | 8          |
| C. Properties of Polymeric Composite Materials.....  | 11         |
| D. Diffusion in Polymers.....                        | 15         |
| <br>   |            |
| <b>III. Experimental Approach.....</b>               | <b>22</b>  |
| A. Materials.....                                    | 22         |
| 1. Monomers.....                                     | 22         |
| 2. Solvent.....                                      | 23         |
| 3. Polyimides.....                                   | 23         |
| 4. Additives.....                                    | 25         |
| B. Sample Preparation.....                           | 27         |
| 1. Polymer Synthesis.....                            | 27         |
| 2. Film Preparation.....                             | 29         |

|            |   |           |
|------------|---|-----------|
| 3.         | Film Modification.....                            | 29        |
| a.         | In-Situ Chemical Generation.....                  | 30        |
| b.         | Infusion Deposition.....                          | 33        |
| C.         | Analysis Techniques.....                          | 36        |
| 1.         | Transmission Electron Microscopy.....             | 36        |
| 2.         | X-Ray Photoelectron Spectroscopy.....             | 38        |
| 3.         | Bulk Elemental Analysis.....                      | 38        |
| 4.         | Thermal Analysis.....                             | 39        |
| <b>IV.</b> | <b>In-Situ Chemical Generation of Dopant.....</b> | <b>40</b> |
| A.         | Introduction.....                                 | 40        |
| B.         | Results and Discussion.....                       | 41        |
| 1.         | Al(acac) <sub>3</sub> as dopant.....              | 41        |
| 2.         | CoCl <sub>2</sub> as dopant.....                  | 51        |
| 3.         | AlO(OH) as dopant.....                            | 62        |
| <b>V.</b>  | <b>Infusion Deposition of Dopant.....</b>         | <b>66</b> |
| A.         | Introduction.....                                 | 66        |
| B.         | Results and Discussion.....                       | 67        |
| 1.         | General Film Properties.....                      | 68        |
| 2.         | AgNO <sub>3</sub> as Dopant.....                  | 74        |
| a.         | Free-standing films.....                          | 74        |
| b.         | Simulated bonds.....                              | 90        |
| 2.         | CoCl <sub>2</sub> as Dopant.....                  | 95        |
| a.         | Free-standing films.....                          | 95        |
| b.         | Simulated bonds.....                              | 97        |

|   |            |
|---|------------|
| <b>VI. Conclusions.....</b>                   | <b>101</b> |
| A. In-Situ Chemical Generation of Dopant..... | 101        |
| B. Infusion Deposition of Dopant.....         | 102        |
| C. Future Work.....                           | 103        |
| <b>VII. References.....</b>                   | <b>104</b> |
| <b>Vita.....</b>                              | <b>109</b> |

## List of Structures

|              |  |    |
|--------------|--|----|
| Structure 1. | 3,3',4,4'-benzophenone tetracarboxylic dianhydride (BTDA)..... | 22 |
| Structure 2. | 1,3-bis(3-aminophenoxy)benzene (APB).....                      | 22 |
| Structure 3. | 4,4'-oxydianiline (ODA).....                                   | 22 |
| Structure 4. | m,m'-diaminobenzophenone (DABP).....                           | 22 |
| Structure 5. | Repeat unit structure of XU-218 polyimide.....                 | 24 |

## List of Illustrations

|            |  |    |
|------------|--|----|
| Figure 1.  | Schematic representation of a microcomposite adhesive bond.....  | 4  |
| Figure 2.  | Thermal expansion coefficient vs. volume % filler for alumina in polyimide BTDA-ODA.....                           | 5  |
| Figure 3.  | General synthesis route for polyimides.....  | 28 |
| Figure 4.  | Schematic of bond arrangement used in adhesive stucy.....  | 32 |
| Figure 5.  | Schematic of "bond" used in initial bondline studies.....  | 34 |
| Figure 6.  | Schematic of "simulated bond" used to monitor dopant movement under bonding conditions.....                        | 37 |
| Figure 7.  | DSC trace of non-modified BTDA-APB.....  | 44 |
| Figure 8.  | DSC trace of Al(acac) <sub>3</sub> modified BTDA-APB.....  | 45 |
| Figure 9.  | Al 2p XPS photopeak from Al(acac) <sub>3</sub> modified BTDA-APB.....  | 47 |
| Figure 10. | C 1s XPS photopeaks from Al(acac) <sub>3</sub> modified BTDA-APB.....  | 50 |
| Figure 11. | Co 2p <sub>(1/2,3/2)</sub> XPS photopeaks from CoCl <sub>2</sub> modified BTDA-APB (film cured through 300°C)..... | 54 |
| Figure 12. | O 1s XPS photopeaks from CoCl <sub>2</sub> modified BTDA-APB (film cured through 300°C).....                       | 56 |
| Figure 13. | Co 2p <sub>(1/2,3/2)</sub> XPS photopeaks from CoCl <sub>2</sub> modified BTDA-APB (film cured through 200°C)..... | 57 |
| Figure 14. | TEM micrograph of CoCl <sub>2</sub> modified BTDA-APB.....   | 60 |
| Figure 15. | TEM micrograph of CoCl <sub>2</sub> modified BTDA-DABP.....  | 61 |
| Figure 16. | TEM micrograph of AlO(OH) modified XU-218...   | 63 |

|            |   |    |
|------------|---|----|
| Figure 17. | TEM micrograph of AlO(OH) modified BTDA-DABP.....   | 64 |
| Figure 18. | TGA trace of AgNO <sub>3</sub> modified BTDA-ODA film cured through 300°C.....  | 70 |
| Figure 19. | TGA trace of AgNO <sub>3</sub> modified BTDA-ODA film cured through 200°C.....  | 72 |
| Figure 20. | TGA trace of AgNO <sub>3</sub> modified BTDA-APB film cured through 200°C.....  | 73 |
| Figure 21. | TEM micrograph of BTDA-ODA film, cured through 200°C, modified with 0.10 M AgNO <sub>3</sub> solution at 100°C.....             | 75 |
| Figure 22. | TEM micrograph of BTDA-APB film, cured through 200°C, modified with 0.10 M AgNO <sub>3</sub> solution at 25°C.....              | 76 |
| Figure 23. | TEM micrograph of BTDA-ODA film, cured through 300°C, modified with 0.10 M AgNO <sub>3</sub> solution at 100°C.....             | 77 |
| Figure 24. | N 1s XPS photopeak from AgNO <sub>3</sub> modified BTDA-ODA.....  | 82 |
| Figure 25. | N 1s XPS photopeak from AgNO <sub>3</sub> modified BTDA-APB.....  | 83 |
| Figure 26. | Ag 3d <sub>(3/2,5/2)</sub> XPS photopeaks from AgNO <sub>3</sub> modified BTDA-ODA.....   | 84 |
| Figure 27. | TEM micrograph depicting the particle distribution in the "simulated bond" using AgNO <sub>3</sub> modified BTDA-ODA films..... | 91 |
| Figure 28. | TEM micrograph depicting the particle distribution in the "simulated bond" using AgNO <sub>3</sub> modified BTDA-APB films..... | 93 |
| Figure 29. | Co 2p <sub>(1/2,3/2)</sub> XPS photopeaks from film modified with CoCl <sub>2</sub> solution.....                               | 98 |
| Figure 30. | O 1s XPS photopeak from film modified with CoCl <sub>2</sub> solution.....  | 99 |

## List of Tables

|          |   |    |
|----------|---|----|
| Table 1. | Film surface atomic percentages and binding energies by XPS for $\text{Al}(\text{acac})_3$ modified BTDA-APB film.....                    | 48 |
| Table 2. | Surface atomic percentages by XPS for BTDA-APB films modified with different amounts of $\text{CoCl}_2$ (1.0X, 0.5X, 0.1X and 0.05X)..... | 53 |
| Table 3. | Peel test results for BTDA-APB films containing variable amounts of $\text{CoCl}_2$ .....   | 58 |
| Table 4. | Elemental Analysis of $\text{AgNO}_3$ modified films....  | 79 |
| Table 5. | Particle sizes in $\text{AgNO}_3$ modified films.....   | 80 |
| Table 6. | Ag $3d_{(3/2,5/2)}$ XPS binding energies and surface atomic percentages in $\text{AgNO}_3$ modified films....                             | 85 |
| Table 7. | Thermal data for $\text{AgNO}_3$ modified films.....  | 89 |
| Table 8. | Dopant particle sizes in "simulated bond" samples.....  | 92 |
| Table 9. | Elemental Analysis of $\text{CoCl}_2$ modified films....  | 96 |

## Chapter I

### Introduction

The use of composite materials with a polymer matrix dates back to at least 5,000 B.C. when pitch was used as a binder for reeds in boat building in the Middle East.<sup>1</sup> Laminated wood veneers have been in use in Greek and Indian cultures for thousands of years. It was not, however, until early in the 20th century that the development of polymeric composite materials began in earnest. In 1909, a composite material of phenol-formaldehyde resin with paper or cloth filler was introduced as Bakelite resin.<sup>1</sup> Later the potential of the polymer resin itself was realized and a rush was on to develop other polymer resins which would be uniquely able to serve as the matrix resins for composite materials.

It was out of this movement that came the development of thermally stable polyimide polymers in the 1950's and early 1960's.<sup>2,3</sup> Thermal stability became a critical factor when it was realized that polymeric composite materials had the potential to replace metals in many structural and aesthetic applications.

Currently, the majority of polyimide composite materials contain fibrous materials as filler material.<sup>4</sup>

These fillers introduce desired mechanical properties such as stiffness and lower thermal coefficients of expansion while maintaining the thermal stability characteristic of the polyimide resin. A major application of these polyimide composites is in the aerospace industry.

In the research and development of polyimide composite materials it was also discovered that using certain metals or metal salts as filler materials resulted in the enhancement of other useful properties of polyimides. These properties included increased thermal stability and even increased adhesive strength.<sup>5-7</sup> Not only have polyimide composites replaced metal as a structural material in some applications, they are also being developed as adhesives to replace traditional metal fasteners such as bolts and rivets. In a recent study by Madigan, metal-modified polyimides were used in an effort to achieve both increased electrical conductivity and effective adhesion of a metal-metal joint.<sup>8</sup>

One of the problems encountered in polymer/metal adhesion is the abrupt change in physical properties at the interface. The adhesive/adherend interface is one of the least understood but most important aspects of adhesive bonding. It is at the interface where the differences between the properties of the adhesive and adherend are brought into sharp focus. For instance, the polyimide

resulting from the condensation reaction between 3,3',4,4'-benzophenone tetracarboxylic dianhydride and 4,4'-oxydianiline (BTDA-ODA) has a linear coefficient of thermal expansion (TCE) of 43 microns/m-<sup>o</sup>C.<sup>9</sup> If this polyimide were to be used as an adhesive for pure aluminum which has a linear TCE of 25 microns/m-<sup>o</sup>C<sup>10</sup>, the integrity of the bond may be threatened if the temperature of the bond varies. The situation is worsened in the case of Al-alloys which have TCE values ranging from 8-12 microns/m-<sup>o</sup>C (ppm). This problem could potentially be alleviated if the adhesive were modified in a controlled fashion such that the TCE and other physical properties changed in a graded rather than abrupt fashion, from the adhesive/adherend interface into the bulk of the adhesive. (see Figures 1 and 2)

The objective of this research was to develop and characterize polyimide/metal or polyimide/metal oxide gradient microcomposite films. The approach involved two different synthetic methods. The first approach was in-situ generation of the modifying specie, an "inside-out" approach. The second method utilized infusion deposition of the modifying material into the film, an "outside-in" approach.

Two different approaches were also taken for determining the existence and nature of the microcomposite structure. The first, an indirect measurement, involved the

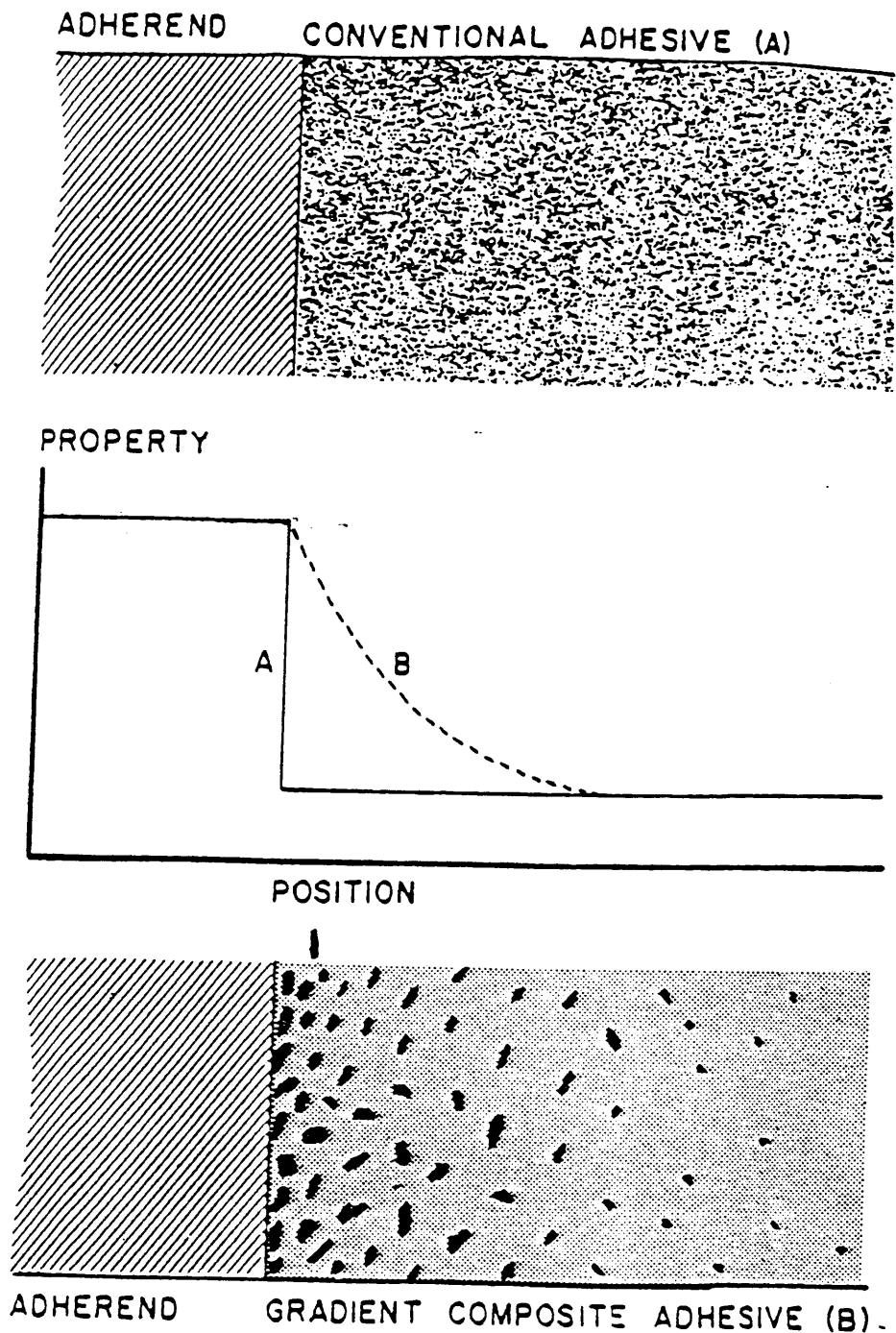


Figure 1. Schematic representation of a microcomposite adhesive bond.

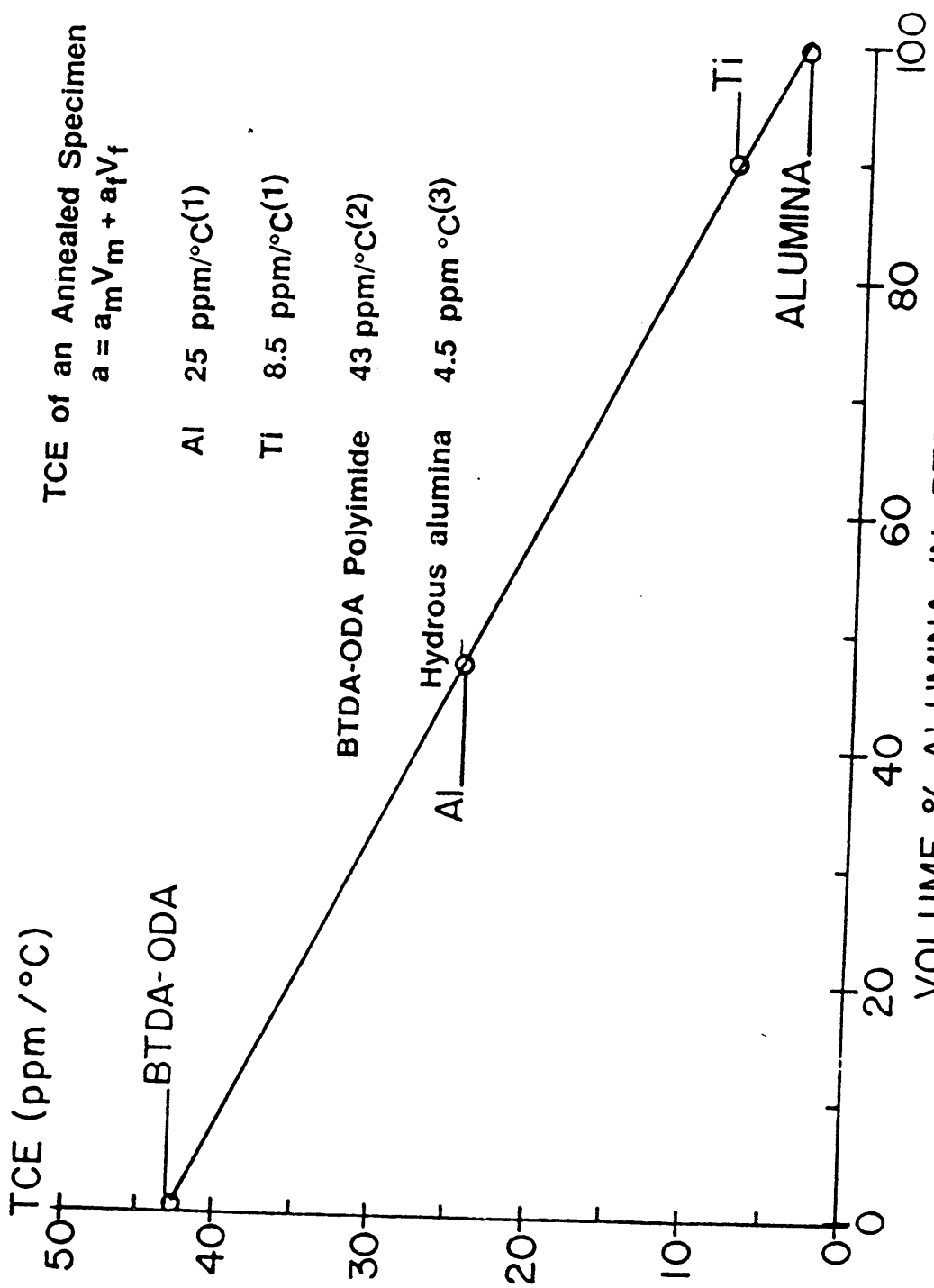


Figure 2. Thermal expansion coefficient vs. volume % filler alumina in polyimide BTDA-ODA.

use of peel tests of adhesively bonded systems. An increase in peel strength would have been used to infer a difference in the physical structure of the thin film adhesive. The second approach was to directly examine cross-sections of the modified polyimide films via transmission electron microscopy (TEM) to determine particle size and distribution within the films. These measurements allow for more accurate observations regarding the feasibility of developing polyimide/metal gradient microcomposite films.

## Chapter II

### Literature Review

#### A. Introduction

There is only a small amount of literature available which deals specifically with the topic of this research; developing controlled gradient microcomposite structures in polyimide films. Thus the nature of this chapter will be to review some of the major principles which support the theory involved and the approaches taken. The history and development of polymeric composite materials in general will be explored. Since a rationale for this work was that a gradient microcomposite material would yield a gradient in physical properties; the effect of fillers and additives on the physical properties of matrix polymers will be addressed as well.

A relatively new approach for modifying polyimide films in this study was infusion deposition. The effectiveness of infusion deposition as a technique depends largely upon the intrinsic properties of the polymer film such as porosity, rate of solvent diffusion through the film and polymer-solvent interactions. Thus the theory of diffusion and absorption in polymers will be investigated as well. This Chapter is not intended to be an exhaustive review of each of the topics mentioned, but rather it will supply the

necessary background for a clearer understanding of the significance of the research.

## **B. Preparation of Polymeric Composite Materials**

Composites are a broad class of materials. Generally composites are defined as combinations of two or more materials present as separate phases, but combined to take advantage of the desirable properties of each component.<sup>11</sup> For the purposes of this thesis, a composite material is further defined to consist of two distinct phases; a major phase, the matrix, and a minor phase, the filler or additive. The discussion will be limited to composites with polymer matrices, hence the term 'polymeric composite materials.'

Even though polymer/fiber composites are the largest class of polymer-based composites, particulate fillers are gaining in importance and useage. These two different types of composites respond to stresses, physical and chemical, in different ways. Thus with good background knowledge and experimentation, composite materials can be prepared which are uniquely suited for specific end-use applications. A factor which would bring an even wider scope to composite preparation would be the ability to control the location and distribution of the filler material in the polymer matrix. For fiber-reinforced materials, that is a fairly

straightforward matter.<sup>12</sup> But for particulate fillers, the situation is much more complex. To further narrow the scope of this Chapter, it is understood that use of the words "filler," "additive" or "dopant" refers to particulate or ionic materials.

There are at least two methods for generating particulate matter in polymer matrices. By far the most popular method involves blending pre-formed particles, ranging from milled metal particles to insoluble inorganic salts, directly into the polymer before it is formed into the final desired product.<sup>13-15</sup> Depending on the mixing technique, one can assume an even dispersion of the filler in the polymer. In some cases, the filler can even aid in the actual processing of the polymer.<sup>16</sup> Chemically treating the filler material is sometimes carried out to yield improved adhesion between the filler particles and the polymer matrix.<sup>17</sup>

Another factor that affects the properties and the synthesis procedure is the size of the filler. According to one researcher, for a material to be called a composite, the reinforcing material must be of a size such that its properties in the composite are what they would be in bulk.<sup>11</sup> This would rule out a large group of modified polymers where metal ions are chelated or otherwise bound to the polymer

backbone.<sup>18-19</sup> In more recent literature, references can be found to polymeric composite materials known as microcomposites, or even nanocomposites.<sup>20-21</sup> The micro- and nano- prefixes refer to the size of the particles in the matrix (i.e. sub-micron sized particles). It is thought that the smaller particles could exert an even greater effect in modifying the properties of the host polymer. The goal of one worker is to develop homogenous composite materials where the filler is molecular in nature.<sup>21</sup>

A key problem in developing microcomposite materials is obtaining filler material in such small sizes. One way to remove that obstacle is to generate the particles chemically in the polymer matrix. Mazur received a patent for a process whereby an inter-layer of silver metal particles is electrochemically generated in a polyimide film.<sup>22</sup> A film is spin-coated on an appropriate cathode. The cathode is immersed in an electrolyte solution which contains salts of metals ( $\text{Ag}^+$ ,  $\text{Cu}^+$  and  $\text{Ag}^+$ ) whose reduction potentials are positive with respect to that from the polymer. When the appropriate potential was applied to the system, metal ions diffused from the solution into the polymer, where they were reduced. Mazur and Reich<sup>23</sup> found that through careful control of the experimental variables of applied potential and metal ion concentration it was possible to control the

location of the metal atom inter-layer. Particles could be generated which were  $< 0.1$  micron in diameter.<sup>23</sup>

Whether particles are chemically generated in-situ or mechanically blended into a polymer matrix, the ultimate goal is still to modify the properties of the polymer.

### **B. Properties of Polymeric Composite Materials**

Thermal, electrical, mechanical, magnetic and optical properties of polymers have been modified by the introduction of particulate matter. Angelo<sup>24</sup> reported one of the first cases of modification of polyimides with a metal compound. Poly(amide acid) was converted to a chelated copper salt. When cast as a film, it was tough and clear brown in color, containing copper particles. Around the same time, Endrey reported forming a conductive polyimide film by incorporating a silver salt. The film contained silver particles of  $< 0.8$  micron in diameter.<sup>25</sup> Workers have developed polyimide/metal(metal oxide) composite films with enhanced thermal, mechanical and electrical properties, specifically increased surface conductivity.<sup>26-31</sup> The surface conductivity is dependent on the existence of a heterogenous composite structure. In other words, the metal particles aggregate at the film surface to render the film an electrical conductor. Process-property studies have shown that process parameters such as curing atmosphere,

polyimide composition, maximum temperature of cure and time of cure all affect whether or not a surface layer of metal or metal oxide forms from the additive.<sup>31</sup>

In a specific case, it was found that the addition of lithium salts to polyimide films sharply increased electrical conductivity and reduced static electricity to virtually zero.<sup>32</sup> The lithium salts were extremely hygroscopic and produced the remarkable electrical changes by adsorbing a layer of atmospheric water on the surface of the film.

Another large class of polymer composite materials is the so-called "engineering materials." These are polymers that are modified by reinforcing material for specific engineering applications. These types of polymeric composites have a long history, and the body of knowledge regarding the subject is vast. The mechanical and thermal properties are well documented for these systems.<sup>33-37</sup>

Stiffness is a major property of polymers that is affected by the inclusion of particulate fillers. Almost universally, a particulate polymer composite material will be stiffer than the neat polymer. Theories abound to explain this, but the common agreement is that the nature of the polymer/ particle interaction is critical. Even though the modulus may increase, tensile strength and elongation at break generally decrease with an increase of filler

concentration. This has been attributed to an increased stress concentration effect.<sup>38</sup> Ohnishi has found that the inclusion of finely divided  $\text{Fe}_2\text{O}_3$  particles in fluorinated polymers increased the adhesive strength of those polymers by an order of magnitude.<sup>20</sup> The effect was concentration dependent. After an optimum loading level of  $\sim 0.05$  volume fraction, the adhesiveness dropped off rapidly, most likely due to increased stiffness of the polymer.

Changes in thermal properties of polymer/particles are also significant. As was mentioned in the Introduction, polymers in general undergo inordinately large thermal expansions during processing and use. The incorporation of fillers tends to decrease the expansion by introducing a different thermal stress distribution pattern. Several thorough review papers are available which take in-depth looks at the various theories that have been put forth regarding thermal expansion in composites.<sup>33-34</sup> In some simple cases, the properties of the polymer and particles are additive, but more often the interaction is much more complex.

Another aspect of thermal properties of composite materials is that of thermal conductivity. Polymers have low thermal conductivities relative to metals. For example, copper has a thermal conductivity of  $400 \text{ Watts meter}^{-1} \text{ Kelvin}^{-1}$ , (W/mK) while polystyrene has a thermal

conductivity of 0.15 W/mK.<sup>1</sup> The Law of Mixtures appears to apply linearly to thermal conductivities of polymer composites. Ziebland has developed an equation which has found good acceptance by other workers.<sup>39</sup>

$$\log k_c = V_p \log k'_p + V_m \log k_m \quad (1)$$

$k_c$  = thermal conductivity of the composite

$k_m$  = thermal conductivity of the matrix

$k'_p$  = hypothetical thermal conductivity of the  
particulate filler

$V_p$  = volume fraction of particulate filler

$V_m$  = volume fraction of polymer matrix

Progelhof et al. have published a review paper on methods for predicting the thermal conductivity of composite systems. In many of the theories presented in that paper, importance was placed on factors such as particle size and shape and particle distributions.<sup>40</sup>

Thermal transitions of polymers, particularly the melting point and glass transition temperature, are also affected by the presence of fillers. The extent of the effect is usually not large. In other words, as the amount of filler increases, the  $T_g$  will increase a few degrees, but will then become constant. However, the heat distortion

temperature, or softening point, usually rises linearly with filler concentration.<sup>1</sup>

In conclusion, it must be emphasized that most of the theory concerning properties of polymer composite materials is based on the assumption of an evenly dispersed filler material. In the event of aggregated particles or stratification of particles, the theories tend to diminish in validity. At that point, theories need to be developed which can focus on molecular interactions and localized polymer/particle interactions.

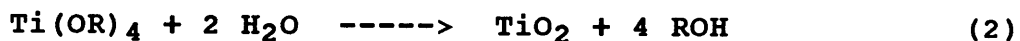
#### **D. Diffusion in Polymers**

Literature on solvent diffusion in polyimides is virtually non-existent. The use of diffusion principles to bring about permanent modification in polyimides is even more rare. The research described in Chapter V of this thesis describes an attempt to prepare composite polyimide films by having the modifying material enter the film via diffusion; being carried into a swollen film by an appropriate solvent.

In 1981, Duchane of the Los Alamos Scientific Laboratory introduced a "novel solvent-based method" that produced super smooth finishes on polymer surfaces.<sup>41</sup> The method involved soaking acrylic rods in a combination of solvent and nonsolvent which would bring about softening and

swelling, but not dissolution of the polymer. As the polymer was swollen both the solvent and the nonsolvent (or penetrant) diffuse into the polymer rod. A simultaneous event is the smoothing of the polymer surface while it is in the "softened" state. In a controlled fashion, the composition of the bath changes, with the solvent gradually being replaced by the nonsolvent. The result is that the solvent is removed from the polymer in a back-diffusion process to maintain equilibrium. The polymer surface becomes rigid again as the solvent is removed and the nonsolvent remains trapped in the polymer. As a result, the surface of the polymer remains smooth after the polymer rod is removed from the solvent-nonsolvent bath. The proper selection of the nonsolvent component will insure a permanent smooth surface on the polymer.

A few years later, Duchane et al. applied the infusion process to bring about surface modification of polymethylmethacrylate rods by a soluble titanium compound.<sup>42</sup> Titanium(IV)isopropoxide served as the nonsolvent in a solvent mixture of isopropyl alcohol and polyvinylpyrrolidone. When the titanium alkoxide diffused into the polymer surface, it was converted to the insoluble titanium dioxide.



Since  $\text{TiO}_2$  is insoluble, it cannot diffuse back out or move about in the polymer. Researchers have shown that surface depositions of titanium oxide can be obtained on polyimide film and silicone sheetstock by soaking these substrates in a solution of titanium tetraethoxide dissolved in dimethylacetamide (DMAc).<sup>43</sup>

To understand why diffusion happens in the first place, it is necessary to understand some of the principles and models that have been applied to the diffusion process. It has been shown that diffusion in glassy polymers, such as polyimides, does not follow the classic theories of diffusion.<sup>44,45</sup> Reasons for this will be presented later. But first it is important to briefly examine the fundamental theories and equations governing diffusion processes.

In isotropic substances, the mathematics of diffusion are based on the premise that the rate of transfer through unit area is proportional to the concentration gradient normal to the area.<sup>46</sup> This can be stated mathematically by:

$$F = -D(\partial C/\partial x) \quad (3)$$

Where:  $F$  = rate of transfer per unit area of section  
 $C$  = concentration of diffusing substance  
 $x$  = space coordinate measured normal to section  
 $D$  = Diffusion coefficient

If it is assumed that diffusion occurs in one direction only, then the differential equation of diffusion is given by:

$$\frac{\partial C}{\partial t} = D \left( \frac{\partial^2 C}{\partial x^2} \right) \quad (4)$$

If, as in many polymer systems, D does not depend on the concentration of the diffusing substance then:

$$\frac{\partial C}{\partial t} = \frac{\partial}{\partial x} (D \frac{\partial C}{\partial x}) \quad (5)$$

Equations 3 and 4 are often referred to as Fick's first and second laws of diffusion.<sup>47</sup> It can be shown then that the sorption of a given penetrant by a homogenous medium is proportional to the square root of the time of diffusion. The ratio of the amount  $M_t$  absorbed at time  $t$  to the amount absorbed at equilibrium  $M_\infty$  is given by

$$M_t/M_\infty = 4/\pi (D \cdot t/l^2)^{1/2} \quad (6)$$

where  $t$  is the time and  $l$  is the thickness of the sheet.<sup>47</sup> Thus a plot of the ratio  $M_t/M_\infty$  would be linear with respect to  $\sqrt{t}$  to the point of equilibrium.

Cases have been reported for the past forty years of solvent-polymer interactions where diffusion did not follow a linear fashion but rather followed sigmoid sorption-desorption curves. That sort of behavior is described as anomalous or "non-Fickian." Non-Fickian behavior is observed in hard or glassy polymers while normal, linear sorption is observed in soft and rubbery materials.

Extrapolating this information to polyimides then, it is possible to conclude that diffusion would occur differently in a polyimide film above and below its glass transition temperature. Kokes found that for polyvinylacetate ( $T_g = 30^\circ\text{C}$ ) sorption above  $30^\circ\text{C}$  gave linear plots versus the square root of time, but sorption curves below  $30^\circ\text{C}$  were sigmoidal.<sup>48</sup> Frisch has described this anomalous diffusion as happening in a two stage process. In the first stage, there is diffusion down a solvent concentration gradient brought about by the instantaneous surface concentration. The second stage then corresponds to sorption with a slowly increasing surface concentration but without a measureable internal concentration gradient.<sup>44</sup>

The major difference then, between diffusion in rubbery polymers and glassy polymers is the response of the polymer to changes in its physical condition. A polymer in its rubbery state responds rapidly to changes in condition brought about by solvent diffusion. On the other hand

glassy polymers respond slowly to changing conditions brought about by the swelling polymer. The slow response-time brings about internal stresses which further affect the extent of diffusion.<sup>49,50</sup> Carbonell et al. have analyzed stresses brought about by that portion of the polymer swollen by the solvent and the glassy part which is unaffected directly by the solvent. In some cases, a sharp, well-defined front is established. As time progresses, the rate of movement of the front decreases and the stress distribution shifts.<sup>51</sup> This applies to solvent diffusing into a polymer.

When the solvent begins to diffuse out of the film, a different dynamic phenomenon is operating. It has been shown that the rate of diffusion out of a glassy polymer is dependent on the history of the solvent movement into the film.<sup>51</sup> Fundamentally, diffusion in polymers is a critical balance between the ability of a polymer to absorb the stresses of swelling by a solvent penetrant and the sorption ability of the solvent. Essentially each polymer/solvent system is a unique situation.

The picture is further complicated if the sorbing solvent is carrying particulate or ionic matter. Interaction of the particles or ions with the polymer can affect the response behavior of the polymer to the solvent. Little is known about the nature of co-diffusion of solvent

and particles through a polymer. Mazur<sup>28</sup> mentions that the diffusion of metal ions through thin polyimide films is Fickian in nature, i.e. the diffusion coefficient of the metal ions is independent of ion concentration. Solvent diffusion in glassy polymers was said to be non-Fickian in nature. Thus it would appear that solvent movement and ion movement through polyimides, at any rate, are independent of each other.

That question could be more thoroughly answered by examining the theories concerning dyeing. Dyeing is in essence a transport phenomena, and is governed by several different processes (i.e. diffusion of the dye through the solvent to the surface of the substrate, adsorption at the surface and diffusion from the surface into the bulk).<sup>52</sup>

The purpose of dyeing is to bring a permanent change to the substrate material. Thus, the interaction between the dye molecule and the substrate must be greater than that between the dye and the solvent. Using these principles to develop predictive models for ion diffusion into polymers would be of great advantage in the attempt to modify polymers in a controlled fashion using diffusion techniques.

## Chapter III

### Experimental Approach

#### A. Materials

A variety of monomers (structures are shown separately) were used to prepare polyimide films which were in one form or another, modified by an array of fillers.

##### 1. Monomers

- a. 3,3',4,4'-benzophenone tetracarboxylic dianhydride  
(BTDA) (Structure 1)

High purity granulated BTDA was supplied by Allco Chemical Corporation (Dallas, TX). It was dried at 100°C under vacuum for three hours prior to use.

- b. 1,3-bis(3-aminophenoxy)benzene (APB) (Structure 2)

APB was supplied by National Starch and Chemical Corporation (Bridgewater, NJ). It was recrystallized in xylene (85°C) and vacuum dried at 80°C for three hours prior to use.

- c. 4,4'-oxydianiline (ODA) (Structure 3)

Zone refined ODA was obtained from Aldrich Chemical Company (Madison, WI) and was vacuum dried at 80°C for three hours prior to use.

d. m,m'-diaminobenzophenone (m,m'-DABP) (Structure 4)

m,m'-DABP was obtained from Aldrich Chemical Company and was vacuum dried at 80°C for three hours prior to use.

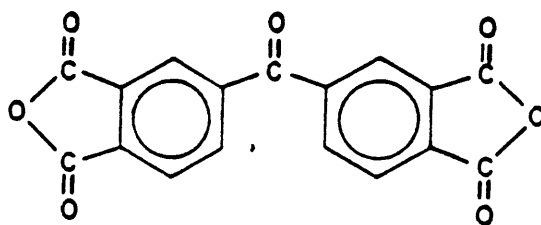
## 2. Solvent

High performance liquid chromatography grade N,N-dimethylacetamide (DMAC) was used as the solvent in the synthesis of the polyimide films used in this study. This solvent was obtained from Aldrich Chemical Company and was used as received. It was stored over 4Å molecular sieves in tightly capped glass bottles.

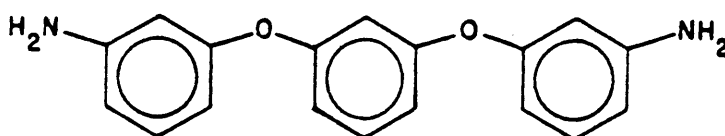
## 3. Polyimides

The two main polyimides of study were formed by reacting the dianhydride BTDA with the diamines ODA and APB respectively. These were chosen for several reasons. They have already been characterized in our laboratory, and the monomers were readily available. There is an appreciable difference in the glass transition temperatures of these two polyimides. BTDA-APB has a  $T_g$  of 200°C while BTDA-ODA has a  $T_g$  of 285°C.

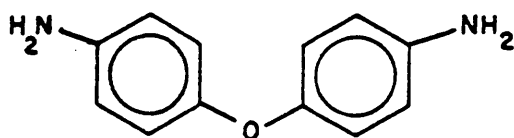
Used on a marginal basis was BTDA-m,m'-DABP ( $T_g = 250^\circ\text{C}$ ) and the soluble polyimide XU-218 ( $T_g = 320^\circ\text{C}$ ).



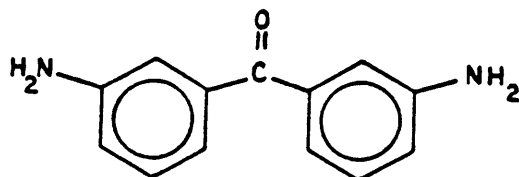
Structure 1. 3,3',4,4'-benzophenone tetracarboxylic dianhydride (BTDA)



Structure 2. 1,3-bis(3-aminophenoxy)benzene (APB)



Structure 3. 4,4'-oxydianiline (ODA)



Structure 4. m,m'-diaminobenzophenone (DABP)

Polyimide XU-218 (Structure 5) was supplied by CIBA-GEIGY Corporation (Hawthorne, NY) and is based on the reaction of BTDA with a proprietary diamine, 5(6)-amino-1-(4'aminophenyl)-1,3,-trimethylindane.

#### 4. Additives

##### a. Tris(acetylacetonato)aluminum(III) - $\text{Al}(\text{acac})_3$

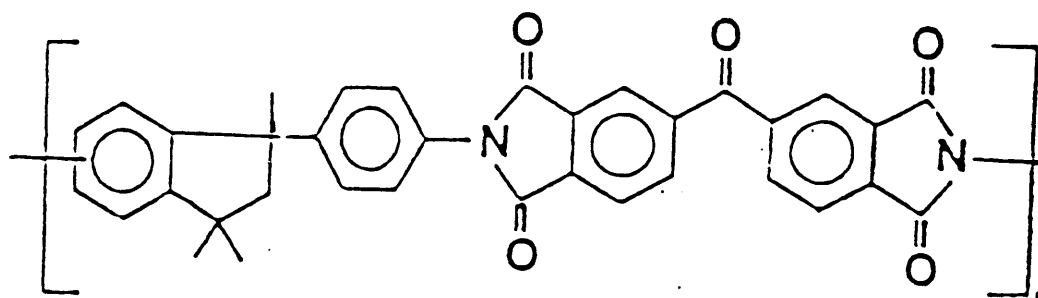
$\text{Al}(\text{acac})_3$  was supplied free from Amspec Chemicals (Gloucester City, NJ) and was used as received. This dopant was highly soluble in DMAC.

##### b. Cobalt(II)chloride - $\text{CoCl}_2$

$\text{CoCl}_2$  was obtained from Aldrich Chemical Company as  $\text{CoCl}_2 \cdot 6\text{H}_2\text{O}$ . It was vacuum dried for 24 hours at  $100^\circ\text{C}$  to remove the waters of hydration. The final form of the additive was a pale-blue powder that was extremely soluble in DMAC.

##### c. Silver(I)nitrate - $\text{AgNO}_3$

$\text{AgNO}_3$  was obtained from Fisher Scientific Company (Fair Lawn, NJ) and used as received.



Structure 5. Repeat unit structure of XU-218 polyimide

d. Aluminum oxyhydroxide - AlO(OH)

AlO(OH) was supplied by Aluminum Corporation of America (Alcoa Center, PA) as a 500Å powder. It was used as received.

**B. Sample Preparation**

1. Polymer Synthesis

The condensation polyimides employed in this study were synthesized in a multi-step process (Figure 3). The diamine was first added to a vented N<sub>2</sub> purged reaction flask with two thirds of the total solvent needed for an 18-20% solids solution. When the diamine was fully dissolved (15 minutes), the dianhydride was added with the remaining solvent, and the solution was mechanically stirred with a Cole/Parmer Master Servodyne stirrer (Cole-Parmer Instrument Co., Chicago IL) at 150 rpm for three hours. The reaction vessel was purged with dry N<sub>2</sub> during stirring. The resultant poly(amide acid) solution was stored under refrigeration until needed.

# polyimide synthesis

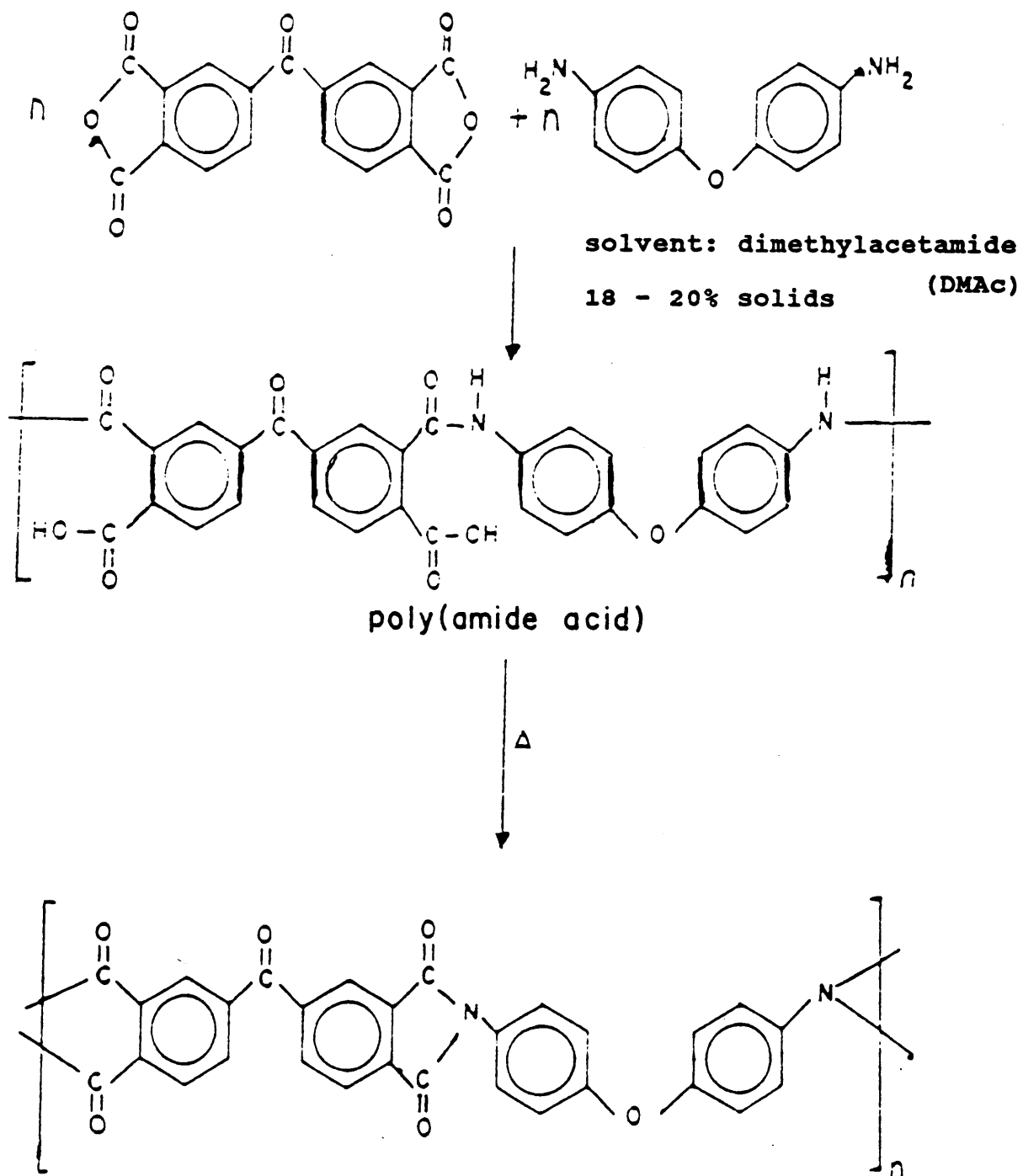


Figure 3. General synthesis route for polyimides

## 2. Film Preparation

All films analyzed in this study were prepared by the same general method. The poly(amide acid) was poured onto a dust-free soda-lime glass plate. A doctor blade, set to a prescribed depth (0.0020"), was then used to draw the solution into a thin film. The film was thermally cured to remove solvent and bring about imidization of the poly(amide acid). A typical cure schedule was one-half hour at 80°C, and one hour each at 100°, 200° and 300°C, all under a dry breathing air atmosphere. After the film was cooled to room temperature, it was removed from the glass plate by scoring the edge of the film with a razor which allowed the film to peel free from the plate.

## 3. Film Modification

Polyimide/metal composite films were synthesized by two separate methods. The first, known as in-situ chemical generation involved introduction of the additive at the poly(amide acid) stage (see Figure 3). The second technique, known as infusion deposition, involved introduction of the additive after the film had been partially imidized.

#### a. In-situ chemical generation

The dopant was added to the reaction flask one hour after both monomers had dissolved and the polyimide precursor, poly(amide acid) had begun to form. Typically, one millimole of dopant was used per four millimoles of monomer, yielding a doping level of "1X." The case of 0.5 millimoles dopant per four millimoles monomer would be designated "0.5X." In this technique, the dopant was homogenously dispersed in the poly(amide acid) solution, but achieved a heterogenous distribution during thermal cure of the polyimide matrix. Much of the in-situ work was conducted in conjunction with a study designed to determine the adhesive properties of the subsequent polyimide metal composite films. To this end, many films were cast on aluminum alloy coupons which were bonded to thin aluminum foil which had been coated with a thin layer of nonmodified polyimide of the same composition. A full report on the adhesive bonding study can be found in the thesis prepared by Laura S. Smith.<sup>53</sup>

A series of BTDA/APB polyimide films modified with either  $\text{CoCl}_2$  or  $\text{Al}(\text{acac})_3$  were prepared. These films were placed in bonding situations by coating 1" x 6" Al7075 coupons with the modified poly(amide acid). The film coat was cured to  $200^\circ\text{C}$ , at which point the film was virtually fully imidized. A bond was made with a piece of high-purity

Al-foil which had on it a thin layer of non-modified BTDA/APB also cured to 200°C (see Figure 4). Bonding took place in a Carver heated hydraulic lab press (Fred W. Carver Company, Menomonee Falls, WI) under the following conditions;

1. Room temperature to 200°C at contact pressure.
2. 200°C for one hour at 500 psi.
3. 300°C for one hour at 500 psi.
4. 300°C to room temperature at 500 psi.

Bonds were tested using a floating roller peel test (ASTM D3167). The failure surfaces were then available for surface analysis.

A second part of the in-situ study involved an attempt to actually determine the bondline structure of the polyimide/metal composite films. Cobalt(II)chloride was used as a dopant because it had a known distribution pattern in free-standing polyimide films. Aluminum-oxyhydroxide was also used as a dopant. Polyimides used in this part of the study were formed by reacting BTDA with APB and m,m'-DABP. The soluble polyimide XU-218 was also used. The variety of polyimides and dopants were used to aid in determining the

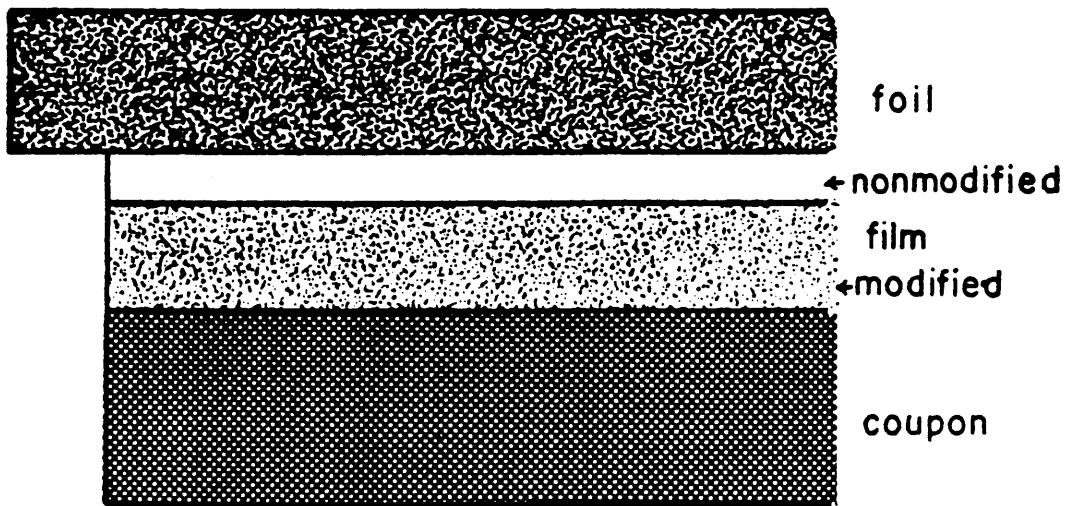


Figure 4. Schematic of bond arrangement used in adhesive studies.

best possible combination to achieve a gradient microcomposite structure in polyimide films.

Films were cast from solution onto glass plates and cured through 200°C. After being removed from the glass plates, the films were placed in the hydraulic press. Temperature and pressure conditions matched those of the bonded specimens mentioned earlier. To achieve a bondline without actually creating a bond, the films were placed between two pieces of Kapton<sup>R</sup> (DuPont) polyimide film, 0.003" and 0.0005" thick (Figure 5). This "sandwich" was placed between two metal coupons and the entire assembly was "bonded." The Kapton<sup>R</sup> film acted as a release agent since it did not adhere to the metal coupons and with some effort could be peeled away from the film sample. The films were then available for analysis by TEM. It must be noted that this technique was carried out under the assumption that the dopant behavior in a bond would not be affected by the nature of the substrate, whether metal or polyimide film. This may not, in fact, actually be the case.

#### b. Infusion deposition

Two polyimides, BTDA/ODA and BTDA/APB and two dopants, AgNO<sub>3</sub> and CoCl<sub>2</sub> were used in this portion of the study. The dopants were dissolved in the solvent used for the polymer synthesis, DMAc. Three different dopant solutions were

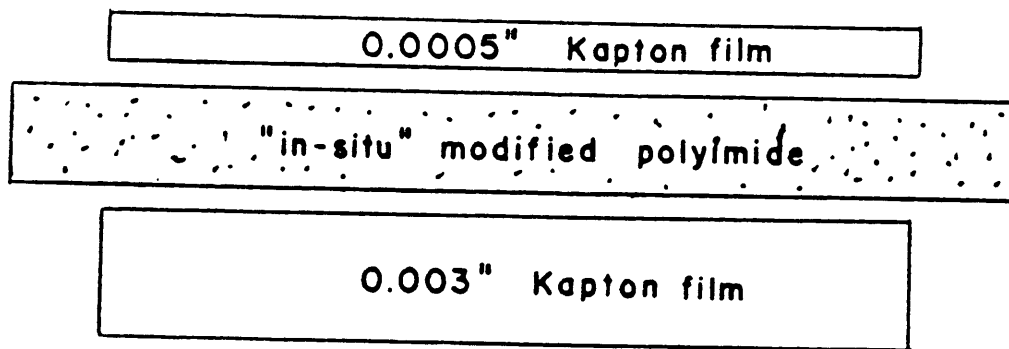


Figure 5. Schematic of "bond" used in initial bondline studies.

prepared; 0.10M, 0.05M and 0.01M. Nonmodified films were cured to 200°C in a dry breathing air atmosphere to remove the bulk of solvent. The films were then removed from the glass plates on which they had been cast and were soaked in the dopant solution. Both BTDA/ODA and BTDA/APB films were soaked in solutions of both dopants at all three concentration levels.

BTDA/ODA films were soaked at 100°C, while BTDA/APB films were soaked at 25°C. Fifty milliliters of solution were used per square inch of film to be soaked. Typically, a 2" x 1" piece of film was soaked in 100-mL of solution in a 250 mL beaker. In the case of the dopant AgNO<sub>3</sub>, care was taken to fully cover the beaker with aluminum foil to prevent photodegradation of silver(I)nitrate. The soaking at elevated temperatures was achieved by suspending the beakers in a water bath. In all cases, soaking took place for one hour after which the pieces of film were immediately removed from the beakers and rinsed with fresh DMAC. The films were put in a Blue-M Touchmaster oven (General Signal Corporation, Wilmington DE) at 100°C and the oven temperature was immediately ramped to 200°C and kept there for one hour. The purpose of this step was to drive off solvent and bring about dopant conversion in the films. The oven was then cooled to room temperature and the films were removed and submitted for analysis.

In addition to free-standing modified film samples, a series of films were retained and used to create "simulated bonds." Since one of the purposes for this research was to develop gradient microcomposite polyimide films which in turn could act as improved adhesives, this part of the study was devised to simulate the behavior of these gradient microcomposite structures in bonding situations. For each dopant and concentration level, two pieces of modified film were retained. These pieces were sandwiched around (air sides in) a piece of non-modified film of the same monomer combination. This tri-layer structure was placed in turn between two pieces of Teflon<sup>R</sup> which acted as release agents (Figure 6). This entire assembly was placed in a Carver heated hydraulic lab press. Each specimen underwent the same "bonding" schedule as was described in section B.3.a. of this Chapter. Cross-sections of these samples were then analyzed by TEM to determine the effect of the "bonding" on the distribution of the microcomposite structure.

## **C. Analysis Techniques**

### **1. Transmission Electron Microscopy (TEM)**

The distribution and particle size of the dopants in the modified films were determined using a Phillips EM-420T

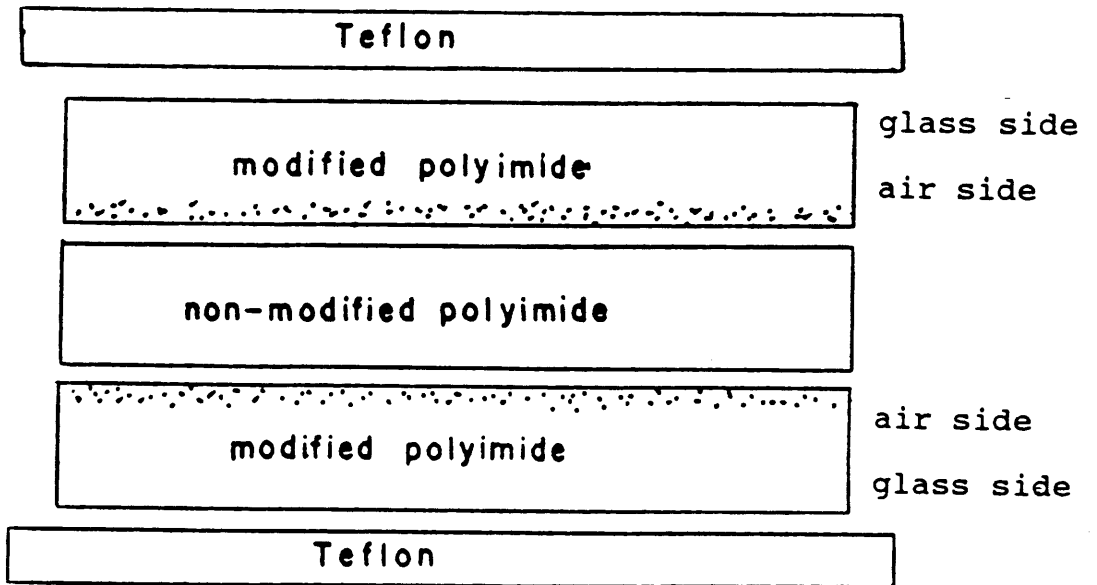


Figure 6. Schematic of "simulated bond" used to monitor dopant movement under bonding conditions.

electron microscope. Photomicrographs of film cross-sections were acquired in the TEM mode. Film samples were prepared by embedding in Polysciences low-viscosity embedding media and cured at 70°C for 24 hours. A Reichert-Jung ultramicrotome was used to cross-section films to a thickness of 1000 Å.

## 2. X-Ray Photoelectron Spectroscopy (XPS)

Film surfaces were analyzed using a Perkin-Elmer PHI 5300 XPS system. A Mg anode (1254 eV) was used at 400 W as the X-ray source, with a spot size of one x three (1x3) millimeters. Film samples were not sputter coated but were fastened to the sample mount using double-stick tape. Survey scans from 0 to 1000 eV were obtained for each sample. Narrow scans were obtained for elements of interest. The instrument was calibrated to a C 1s binding energy of 284.6 eV, and the reported error in the binding energies is  $\pm 0.2$  eV. Values reported are single analyses.

## 3. Bulk Elemental Analysis

Elemental analyses of films were performed by Galbraith Laboratories, Inc, (Knoxville, TN). Single analyses were done on films modified by AgNO<sub>3</sub> and CoCl<sub>2</sub> in the infusion

deposition process. No elemental analyses were carried out on films modified by the in-situ method.

#### 4. Thermal Analysis

A Perkin-Elmer TGS-2 thermal analyzer was used to obtain thermogravimetric analysis (TGA) data and a Perkin-Elmer DSC-4 instrument was used to obtain differential scanning calorimetry (DSC) data on the film specimens. A Perkin-Elmer System 4 Thermal Analysis Data Station was used to evaluate the data. The polymer decomposition temperature (PDT) taken at 10% film mass loss, was obtained from the TGA experiment which incorporated a dry breathing air atmosphere and a heating rate of 20°C/minute. Glass transition temperatures were obtained from the DSC data with a nitrogen atmosphere and a heating rate of 20°C/minute.

## Chapter IV

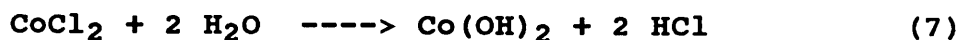
### In-Situ Chemical Generation of Dopant

#### A. Introduction

In the fabrication of metal/metal composites, a common technique used is that of in-situ growth, where the reinforcing phase is produced simultaneously with the matrix. This technique contrasts with the more conventional approach of forming the matrix and filler in separate processes.<sup>54</sup>

In previous research the formation of composites with organic polymer matrices and inorganic fillers most often takes the in-situ approach. The research presented in this Chapter is a study of the behavior of inorganic [CoCl<sub>2</sub>, AlO(OH)] and organometallic [Al(acac)<sub>3</sub>] fillers in aromatic poly(amide acid) matrices, during the curing process. In this context, the dopant precipitates and migrates simultaneously with imidization. In this regard, Madeleine has studied the in-situ growth of gold particles in polyimide films.<sup>55</sup> In this study the focus is more on the final distribution pattern of dopant particles than on the actual growth of the dopant specie. It must be kept in mind, however, that the final distribution of particles is affected by the nature of particulate nucleation and growth.

In addition to the physical processes that affect the growth of the dopant material, concomitant chemical changes also take place. A common chemical reaction that takes place is hydrolysis/dehydration of metallic species at the film surfaces. For example:



For two of the dopants,  $\text{CoCl}_2$  and  $\text{Al(acac)}_3$ , it was hoped that there would be a conversion to the oxide forms, as the oxides are inherently more stable than the initial species. The third dopant,  $\text{AlO(OH)}$  was used to determine the feasibility of initially dispersing an oxide form in the poly(amide acid).

## B. Results and Discussion

### 1. $\text{Al(acac)}_3$ as the dopant

A previous study by Taylor and St.Clair gave evidence that the use of  $\text{Al(aca)}_3$  as a dopant in the polyimide BTDA-*m,m'*-DABP resulted in increased adhesive strength (lap shear mode) at elevated temperatures.<sup>5</sup> The rationale presented at that time for the increased strength was that the presence of the dopant increased the softening temperature of the

polymer. Nothing was suggested regarding the exact nature of the dopant distribution. Since the lap shear test measures fundamentally the bulk properties of an adhesive, it was assumed that the dopant was evenly dispersed in the bulk of the film. With this information in mind, the decision was made to use  $\text{Al}(\text{acac})_3$  as a dopant in this study. Even though the test mode would be quite different (room temperature peel testing), the logic presupposed that the dopant would behave in the desired fashion (i.e. migrate to near the film interface and form there a microcomposite structure).

The presence of  $\text{Al}(\text{acac})_3$  in BTDA-APB was found to exert a wide range of effects on the film properties, relative to nonmodified BTDA-APB. Free-standing films which had been modified and were cured through  $300^\circ\text{C}$  were brown in color. A nonmodified, fully cured BTDA-APB film was light yellow. When the dopant was first added to the poly(amide acid) solution, the color remained a clear light yellow. During the thermal cure process of a film, the color gradually changed to the dark brown color. This color change indicated that either 1) the dopant converted to another form, 2) coordination of the dopant with the polyimide backbone, 3) the dopant remained in its original chemical state and just migrated to the surface and formed a dense layer of dopant material there, or 4) the aluminum ion

catalyzed some polyimide decomposition. As such, the color change did not give any direct evidence that the desired gradient microcomposite structure had formed.

Thermal analysis of these films indicated that the presence of the dopant increased the glass transition temperature of BTDA-APB. As seen in Figures 7 and 8 respectively, the  $T_g$  of nonmodified BTDA-APB is  $198^\circ\text{C}$  while the  $T_g$  for BTDA-APB//Al(acac)<sub>3</sub> is  $224^\circ\text{C}$ . The  $26^\circ$  difference suggests there was some polymer/dopant interaction. The PDT for the modified film was not changed significantly from that of nonmodified BTDA-APB. Often the presence of metal, metal salts or organometallic compounds will lower the thermal stability of the composite material, possibly through a catalytic effect due to the presence of the metal specie. In the case of BTDA-APB//Al(acac)<sub>3</sub>, however, an increase in thermooxidative degradation was not seen. Thus the stiffness of the polymer was increased without sacrificing thermal stability.

In polymer composite materials, both the location and chemical state of the dopant can affect the overall properties. It was hoped that the Al(acac)<sub>3</sub> would convert to Al<sub>2</sub>O<sub>3</sub> in the polyimide film near the film surface, and thus provide a thermally stable microcomposite structure, which would increase the adhesive nature of BTDA-APB. But first

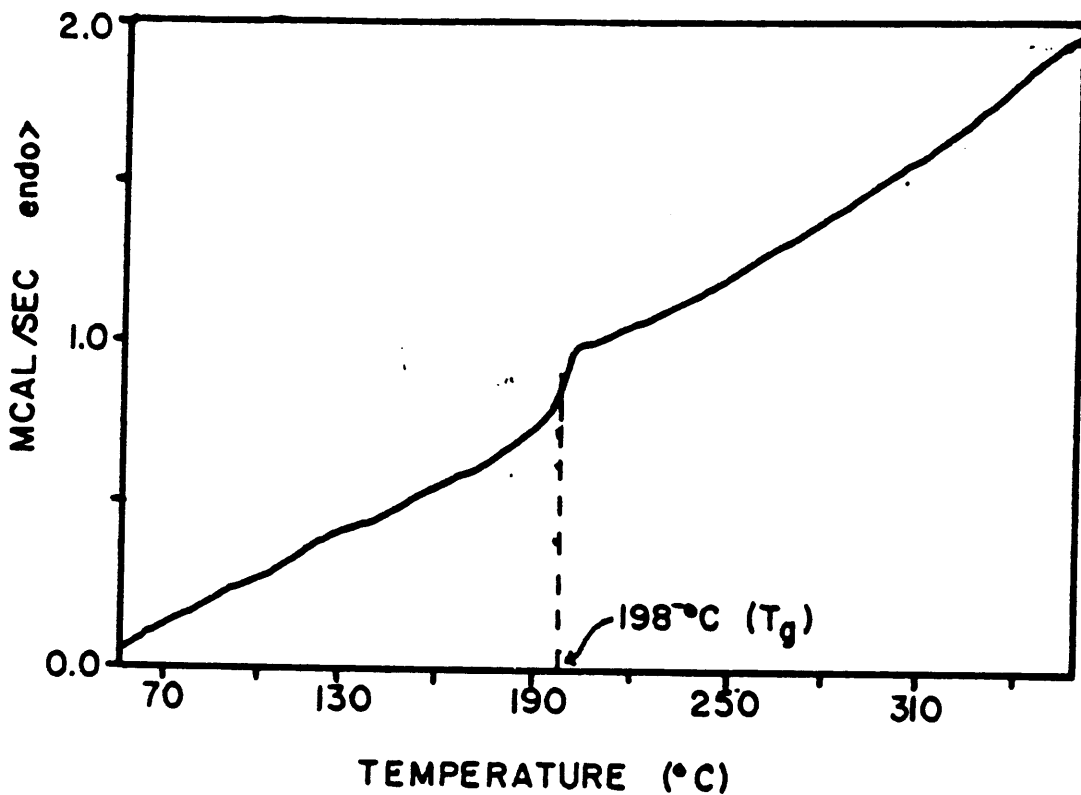


Figure 7. DSC trace of nonmodified BTDA-APB.  
(dotted line indicates glass transition)

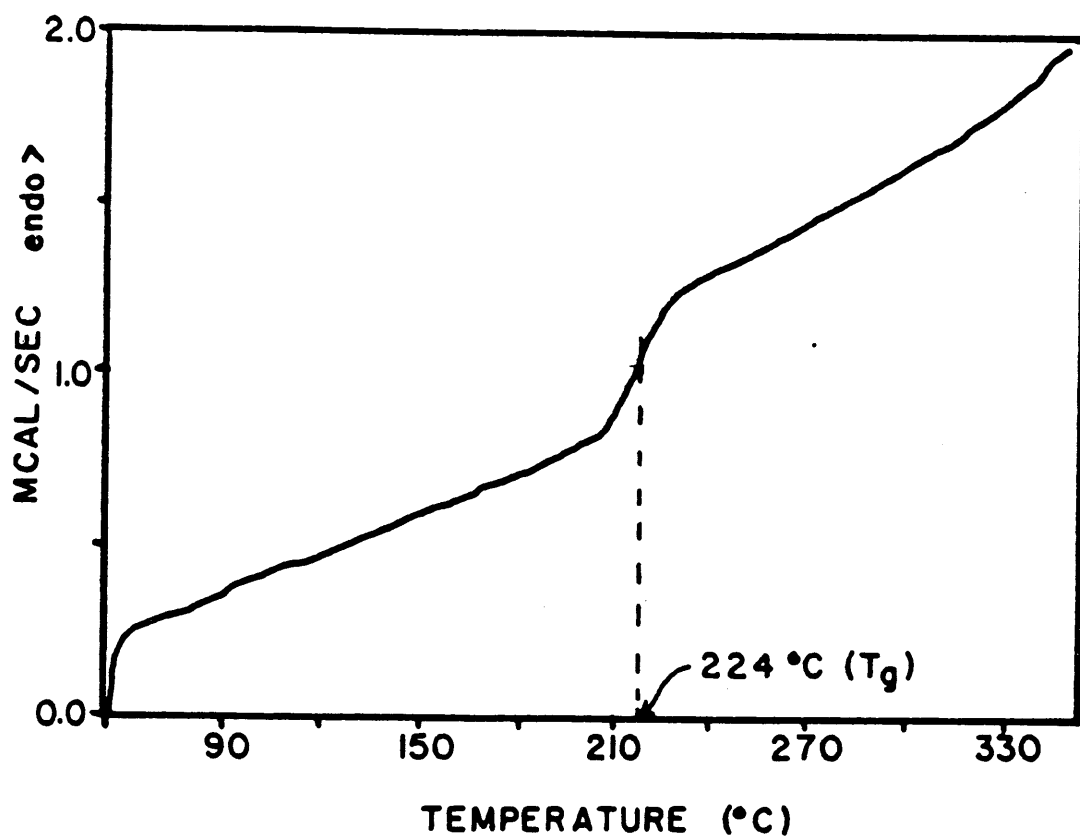


Figure 8. DSC trace of  $\text{Al}(\text{acac})_3$  modified BTDA-APB. (dotted line indicates glass transition)

free-standing films were analyzed by XPS to determine the nature of the dopant at the surface.

Both the air side and glass side of a free-standing  $\text{Al}(\text{acac})_3$  modified BTDA-APB film were analyzed. Virtually no aluminum was seen on the glass side of the film, so data presented is from the air side. The Al 2p photopeak binding energy was 74.3 eV, indicative of the  $\text{Al}^{3+}$  specie (Figure 9). If any aluminum metal had been present, it would appear at a lower binding energy, around 72.0 eV.

Table 1 lists the relative atomic percentages and the corrected binding energies for both a modified film and a nonmodified film. The amount of aluminum on the surface of the modified film is significant relative to an initial uniform distribution of dopant. Given that the amount of dopant initially in the film was one millimole per four millimoles of monomer and that the expected C:N:O ratio for BTDA-APB is 35:2:7 (per repeat unit) and assuming a homogenous dispersion, the Al:N ratio should be 1:8. Instead the Al:N ratio is 1:2, indicating that the dopant had segregated preferentially toward the "air" surface. Nitrogen was used as a tag atom because rarely is excess nitrogen introduced from contamination. This data would suggest a gradient had formed, with a surface rich in dopant material. TEM analysis of these modified films, however, did

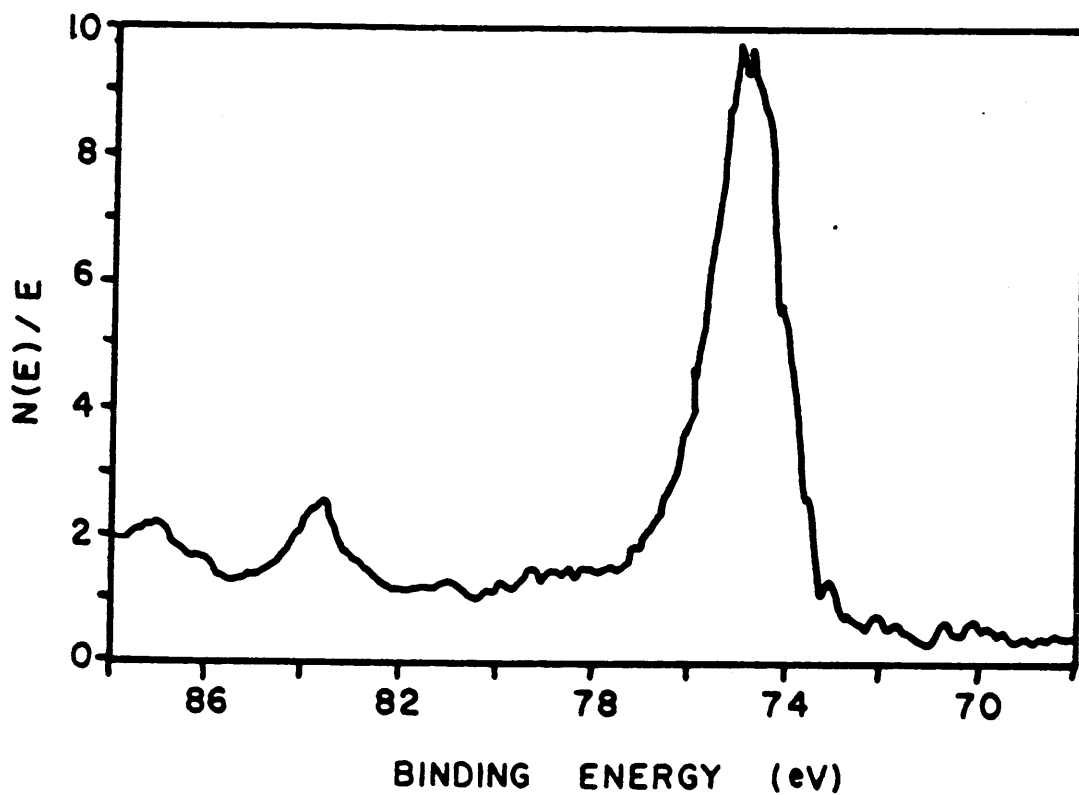


Figure 9. Al 2p spectrum from  $\text{Al}(\text{acac})_3$  modified BTDA-APB.

**Table 1**

Film surface atomic percentages and binding energies by XPS for Al(acac)<sub>3</sub> modified BTDA/APB film

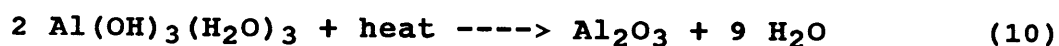
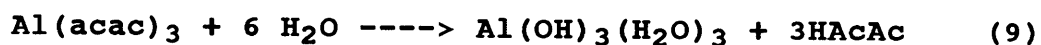
| <u>element</u> | <u>atomic %</u> | <u>binding energy (eV)</u> |
|----------------|-----------------|----------------------------|
| C              | 72.4            | 284.6, 288.2               |
| O              | 20.2            | 531.6                      |
| N              | 4.8             | 400.0                      |
| Al             | 2.6             | 74.3                       |

not reveal any such gradient microcomposite structure.

The question still remains as to whether the Al on the film surface is unchanged dopant, or Al<sub>2</sub>O<sub>3</sub>. This question could be answered by comparing the C 1s photopeaks and binding energies of the modified and non-modified films. If the dopant were still present as Al(acac)<sub>3</sub>, one would expect to see a difference in the C 1s carbonyl peak from the acac ligand. The peaks are virtually identical (see Figure 10). However, keeping in mind the small amount of Al actually on the surface of the film, it can be expected that any change in the carbon distribution would not actually be noticeable.

It is possible that the dopant has converted to another form, possibly Al<sub>2</sub>O<sub>3</sub>. The presence of an O1s oxide peak would confirm that theory. Unfortunately the O1s oxide peak has nearly the identical binding energy as that of the O1s imide oxygen. However, full-width half-maximum (FWHM) measurements revealed an increase of 0.4 eV in the O1s photopeak of the modified film, most likely a result of existence of O1s oxide oxygen.

A search of the literature did not reveal a mechanism for the reaction Al(acac)<sub>3</sub> ----> Al<sub>2</sub>O<sub>3</sub>, but a plausible reaction scheme can be envisioned as follows:



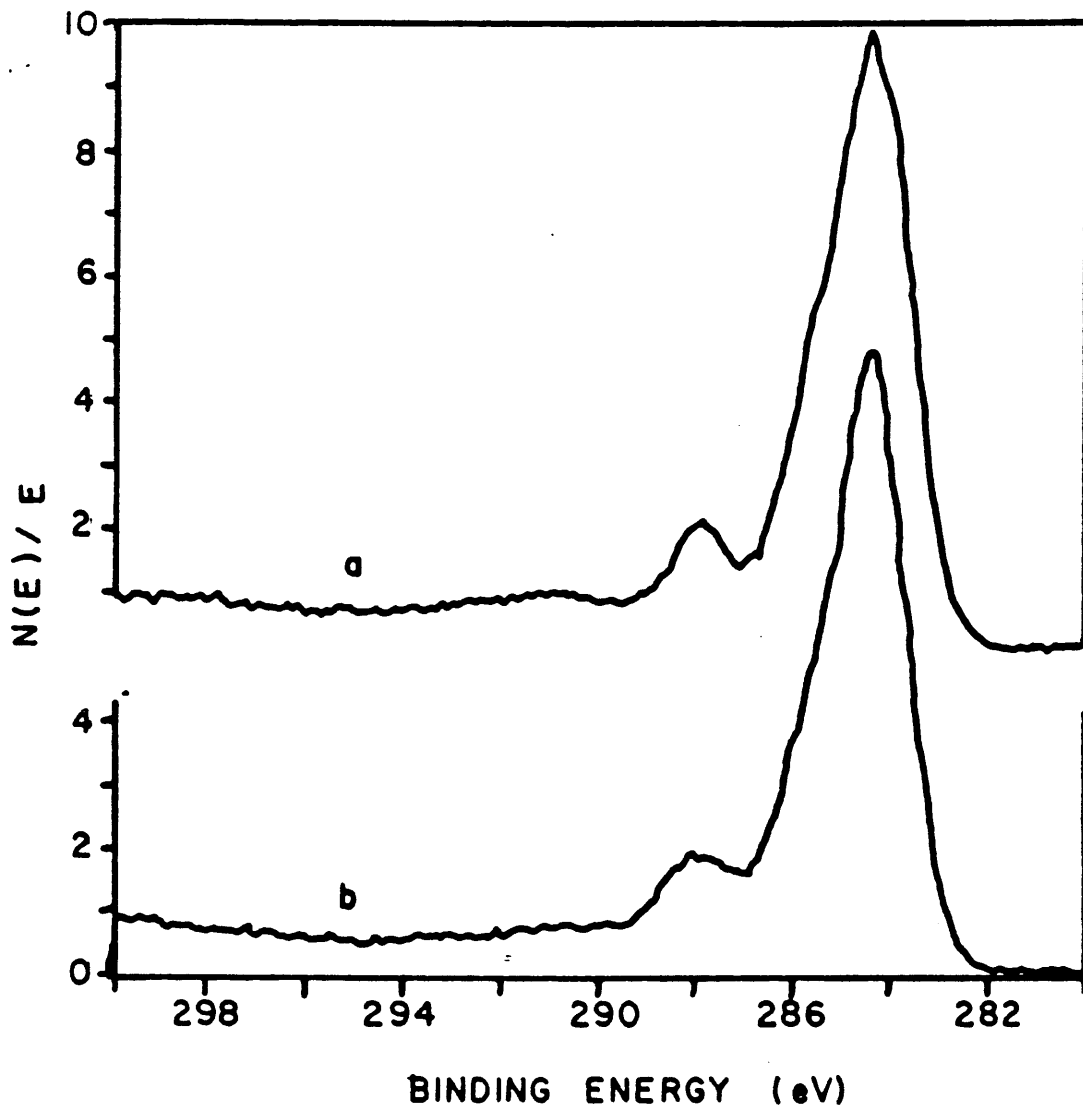


Figure 10. C 1s XPS photopeaks a) nonmodified film, b) Al(acac)<sub>3</sub> modified film.

A primary goal of this aspect of the thesis was to determine if the modified films would affect the adhesive properties of BTDA/APB in a positive fashion (i.e. increase the peel strength). More concretely the question can be asked if the presence of  $\text{Al}_2\text{O}_3$  at the surface of a modified BTDA-APB film would affect the adhesive nature of the film.

The results of the floating roller peel test of bonded specimens with  $\text{Al}(\text{acac})_3$  modified adhesive indicated that the dopant was acting to form a weak boundary layer in the bond and thus decrease the overall adhesive strength of BTDA-APB. Two sets of peel test samples were prepared; one with non-modified adhesive, the other with modified adhesive. Under identical bonding and testing parameters, the modified adhesive gave a peel strength of 7.0 Newtons/cm (N/cm) while the non-modified adhesive gave a peel strength of 17 N/cm. Obviously the modified adhesive in this case apparently did not produce a gradient microcomposite structure which could act to increase the peel strength of BTDA-APB polyimide.

## 2. $\text{CoCl}_2$ as the dopant

The next step using the in-situ approach was to use a dopant which had a proven migration behavior pattern in polyimide matrices. Taylor et al. have produced a series of

papers characterizing cobalt modified polyimides,<sup>56-61</sup> therefore cobalt(II)chloride became an obvious choice as a dopant in this study. In addition, a rationale for using  $\text{CoCl}_2$  as a dopant was that it would allow a more direct correlation between the distribution of the dopant material in a thin modified free-standing film and the adhesive peel strength of that same film.

A first experiment was to vary the concentration of the dopant to determine if the concentration level affected the amount of material which could migrate to the surface of the cured film and potentially form a gradient interface. Four films were cast on coupon material with dopant concentrations of 1.0X, 0.5X, 0.1X and 0.05X, respectively. Table 2 lists the cobalt concentrations employed with film surface atom percentages. It is quite evident that there is in fact a trend in the surface concentration of cobalt at the surface of the fully cured films with the cobalt chloride doping level.

The XPS results for these films indicated that Co was present mostly as Co(III), with a small amount of Co(II) as well. The Co  $2p_{1/2,3/2}$  photopeaks (Figure 11) show a peak separation of nearly 16 eV, indicative of the Co(III) state. The presence of satellite peaks is indicative, though, of some Co(II) present. The Co is present then most likely as

**Table 2**

Surface atomic percentages by XPS for BTDA/APB films modified with different amounts of  $\text{CoCl}_2$  (1.0X, 0.5X, 0.1X and 0.05X).

| elements | <u>atomic percentages</u> |      |      |       |
|----------|---------------------------|------|------|-------|
|          | 1.0X                      | 0.5X | 0.1X | 0.05X |
| C        | 32.3                      | 37.4 | 63.0 | 76.0  |
| O        | 33.6                      | 35.8 | 22.5 | 18.7  |
| N        | 0.7                       | 1.1  | 3.9  | 5.0   |
| Co       | 24.5                      | 22.4 | 8.9  | 0.3   |
| Cl       | 8.9                       | 3.3  | 1.7  | 0.0   |

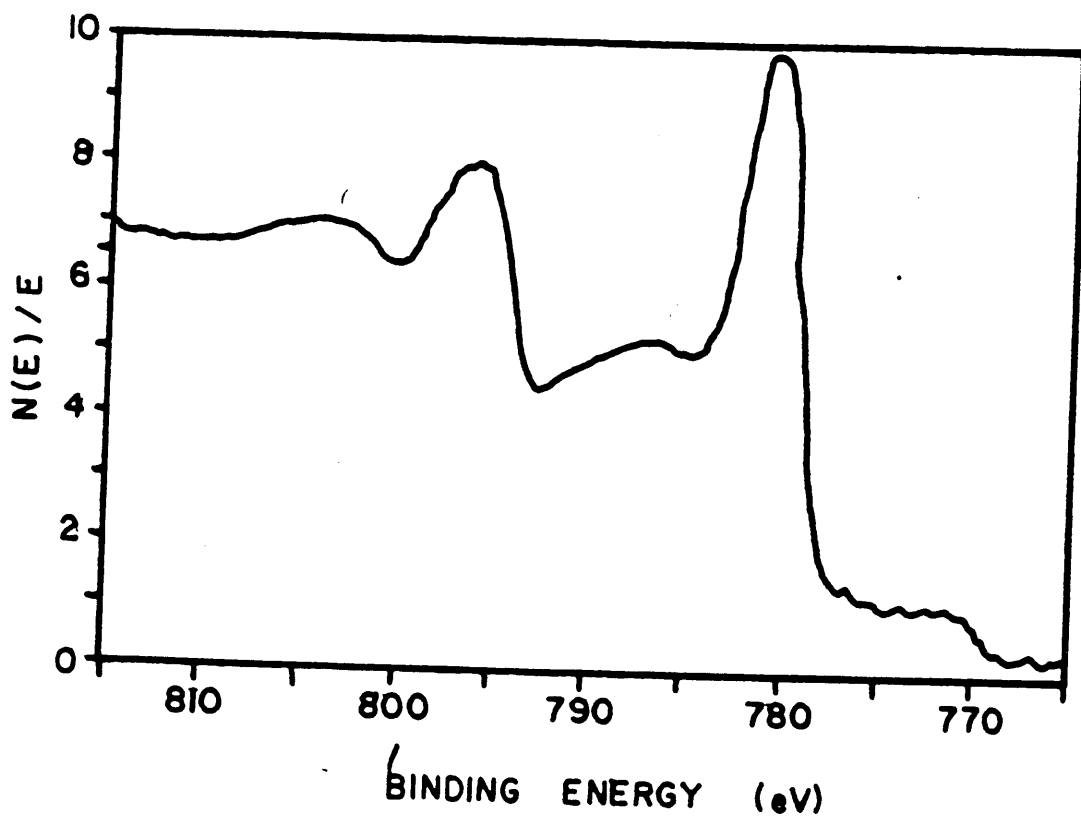


Figure 11. Co 2p(1/2, 3/2) XPS photopeaks.  
(film cured through 300°C)

the mixed oxide  $\text{Co}_3\text{O}_4$ . The O 1s photopeaks (Figure 12) support this conclusion by the presence of a distinct O1s oxide peak on the low binding energy side of the O 1s imide oxygen peak.

Although there seemed to be a surface-rich type of composite structure for these fully cured films, the next step was to take films of variable dopant concentration and apply them as adhesives. For this purpose the films were cured to only  $200^\circ\text{C}$  to assure better flow and better contact with the other adherend. XPS results indicate that at this stage, the cobalt still migrated to the surface, but not in as large a quantity. The Co  $2p_{1/2,3/2}$  photopeaks (Figure 13) indicate cobalt was exclusively in the Co(II) state, as evidenced by the noticeable satellite structure.

The adhesive peel strengths for the variable dopant concentrations are listed in Table 3. There is not a trend in peel strength with respect to dopant concentration and apparently the dopant does not form a gradient micro-composite structure which could act to increase the adhesive nature of BTDA/APB. It was noticed however that the cobalt dopant does migrate through the non-modified layer of BTDA/APB which had been coated on the foil adherend. XPS analysis of failed surfaces (i.e. the samples which failed at the foil/adhesive interface) revealed small amounts of cobalt(II) on both the foil surface and the adhesive

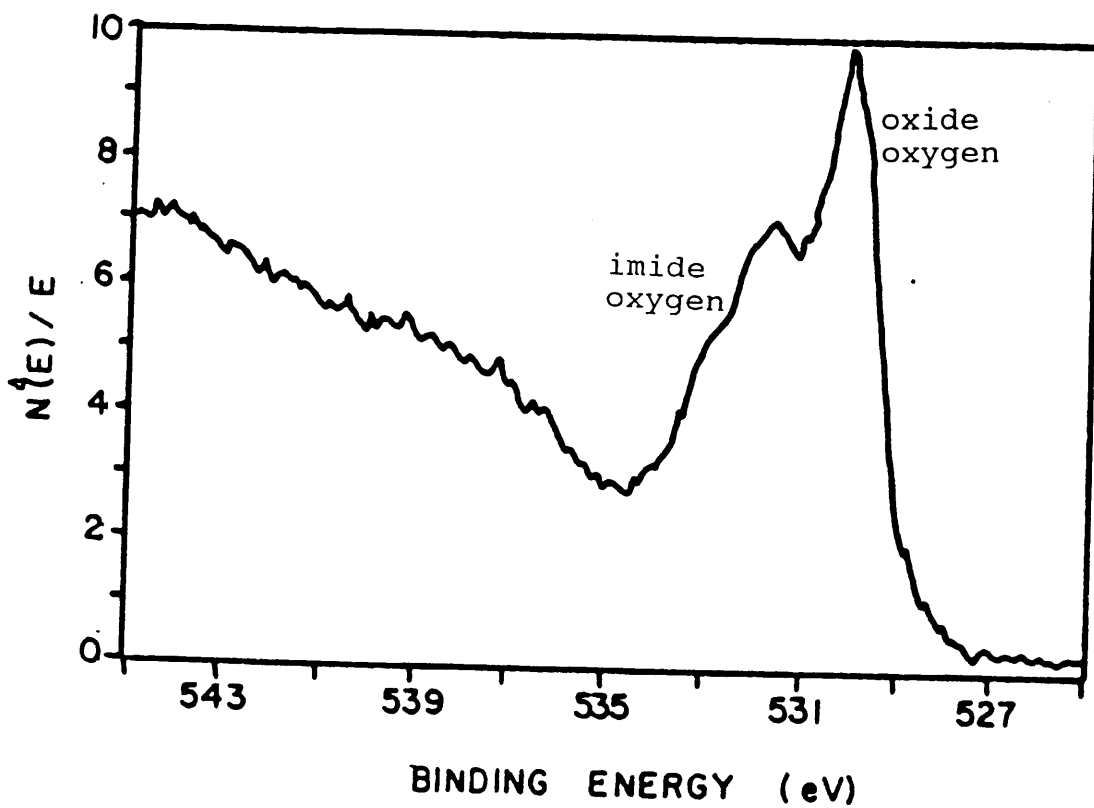


Figure 12. O 1s XPS photopeaks (from imide oxygen and oxide oxygen).

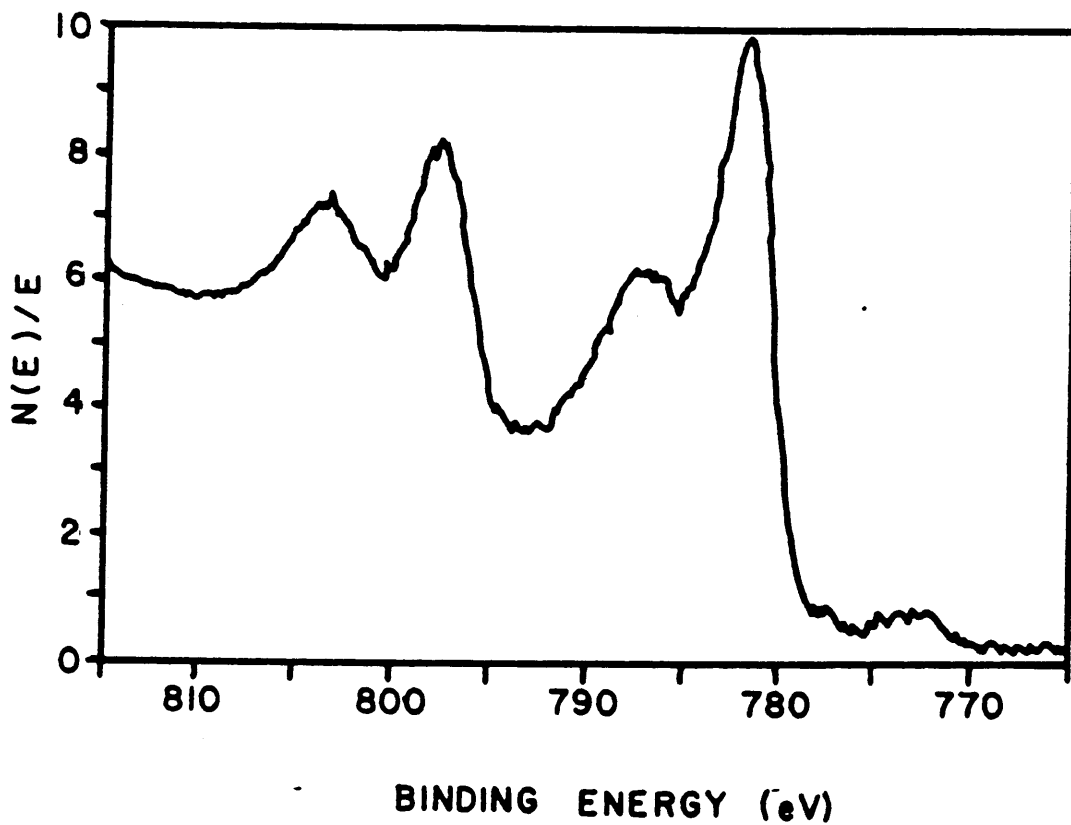


Figure 13. Co 2p(1/2,3/2) XPS photopeaks.  
(film cured through 200°C)

**Table 3**

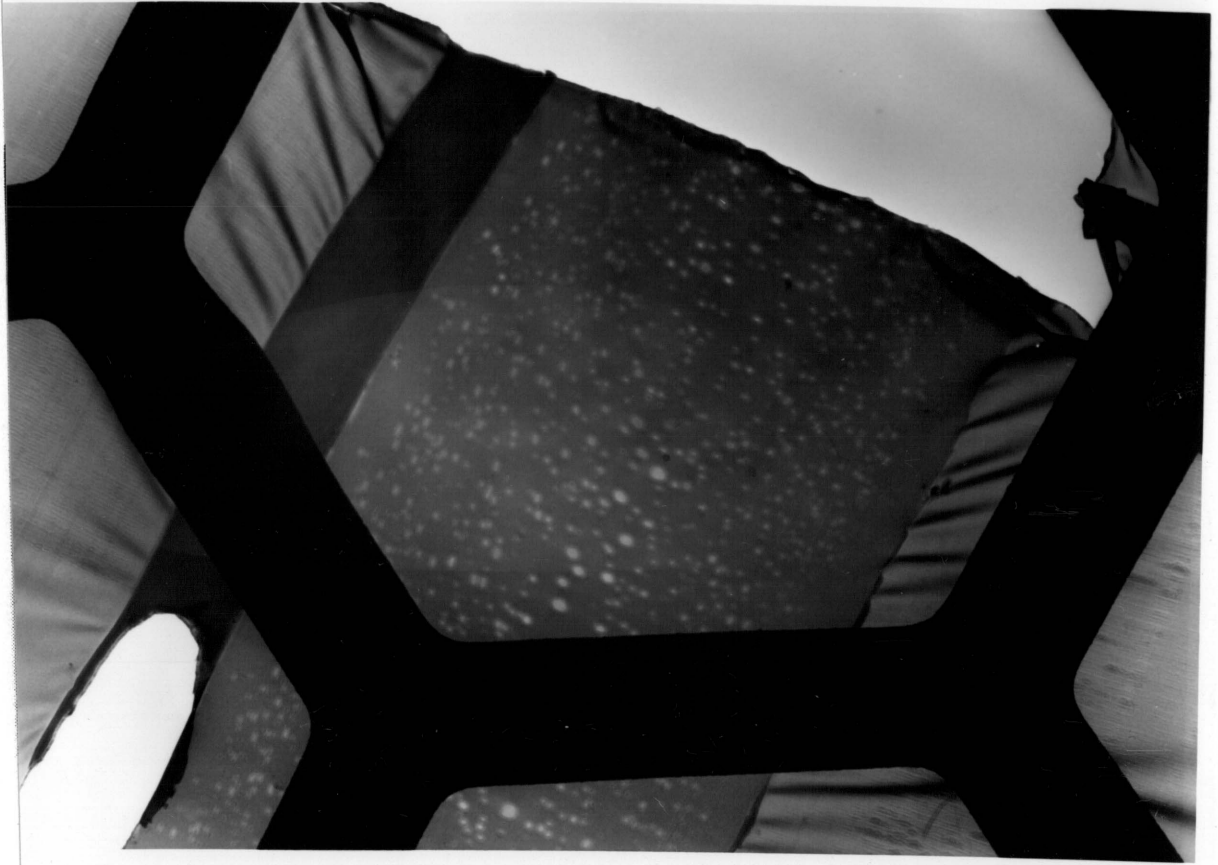
Peel test results for BTDA/APB films with variable dopant levels of  $\text{CoCl}_2$ .

| <u>dopant concentration</u> | <u>peel strength (N/cm)</u> |
|-----------------------------|-----------------------------|
| undoped                     | 5.3                         |
| 0.05X                       | 5.8                         |
| 0.10X                       | 5.3                         |
| 0.50X                       | 5.1                         |
| 1.00X                       | 5.3                         |

surface. This indicated that the dopant had not undergone any chemical conversion during the bonding process. Although this result was expected, it still yielded valuable information (e.g. dopant migrating through nonmodified polyimide) toward the understanding of dopant behavior in polyimides during adhesive applications.

To extend that understanding, two polyimides, BTDA-APB and BTDA-*m,m'*-DABP, were modified with  $\text{CoCl}_2$  with the in-situ approach and subjected to the pressure and temperature of an actual bond. TEM was used to analyze the films which had been "bonded." Figures 14 and 15 are representative pictures of cross-sections of BTDA-APB and BTDA-*m,m'*-DABP films, respectively.

The most striking feature in the BTDA-APB films was the apparent absence of dopant in the film. It is theorized that the holes in the film is where the dopant particles had been. Apparently during the preparation of the film sample for TEM analysis, the dopant material dissolved out of the film. The most likely situation for that to have happened was during the microtoming. As the film cross-sections are cut off, they are floated on water, where the  $\text{CoCl}_2$  that is exposed dissolves away. Even so, the holes gave an idea of the distribution of the particles in the film. Although the holes are fairly uniform in size, there is a "depletion zone" near the edges of the film. That was a somewhat



magnification: 1640X

10 um



Figure 14. TEM micrograph of  $\text{CoCl}_2$  modified BTDA/APB.



magnification: 2760X

5 um  
┌────────┐

Figure 15. TEM micrograph of  $\text{CoCl}_2$  modified BTDA/DABP.

different result than would have been expected from the XPS data given earlier where there was shown to be a large degree of cobalt enrichment at the film surface. The depletion zone likely came about as a result of dopant particles diffusing into the Kapton<sup>R</sup> film which had acted as the release agent.

The obvious difference noted in the BTDA-m,m'-DABP film is that dopant particles are present. There appears to be an even distribution of particles across the breadth of this film, all of relatively large size. Most of the particles are in the range of 0.2 - 0.6 micron diameter. Overall, the force of pressure and temperature for this film had the effect of "enforcing" a relatively uniform distribution of dopant material throughout the film. Although it could still be termed a 'composite material', a gradient microcomposite structure is not in place.

### 3. AlO(OH) as dopant

Two different polyimides were used in this part of the study, one soluble pre-imidized polyimide XU-218 and BTDA-m,m'-DABP. The results by TEM analysis were virtually identical (Figures 16 and 17). In both cases, the dopant aggregated into large clumps within the bulk of the film, with no apparent migration to either surface. Although the dopant was not completely dispersed in the polymer



magnification: 2790x

5  $\mu\text{m}$



Figure 16. TEM micrograph of  $\text{AlO}(\text{OH})$  modified XU-218.



magnification: 2,760X

5  $\mu\text{m}$



Figure 17. TEM micrograph of  $\text{AlO}(\text{OH})$  modified BTDA/DABP.

solutions use of an ultrasonic bath helped achieve a homogenous dispersion. The dopant did not remain dispersed because of surface energy considerations which drove the AlO(OH) to aggregate rather than remain dispersed. If an electronic charge (peptisation) could have been applied to the surface of the AlO(OH) particles (500Å) through the judicious use of counter ions in the solvent, the particles would have remained in a dispersed state because of the oppositional forces of the counter ions and possibly generated a gradient microcomposite structure.

## Chapter V

### Infusion Deposition of Dopant

#### A. Introduction

One of the findings presented in Chapter IV was that dopant material will migrate, or diffuse, from a modified film into a non-modified film when the two are placed in contact with each other under bonding conditions. The significance of that finding is that if the diffusion could be controlled in some manner, a concentration gradient of dopant particles could be realized near the film surface, to form a desired interphase. The interphase can be described as that area from the film surface into the film which is affected in some way (physically or chemically) by the presence of a modifying or reinforcing agent.

The objective of this research was to create polyimide films where only the near surface areas were modified by the dopant. The first approach, outlined in Chapter IV involved homogenous saturation of a film with dopant by having the dopant dissolved in the poly(amide acid). The envisioned result was that the gradient microcomposite structure would spontaneously form near the surfaces of the film.

The second approach details a completely different tactic wherein the dopant is intentionally deposited near the surface of a polyimide film. The extent of any gradient formation is controlled by the kinetics and thermodynamics of the diffusion process. Infusion deposition is fundamentally a diffusion and absorption phenomena. Results will also indicate that temperature and degree of imidization of the film also affect the formation of a gradient microcomposite interphase. The nature and concentration of the dopant material affected the overall microcomposite structure as well. In essence, if each of the factors mentioned could be carefully optimized, much more structural control could be had.

The technique of creating a polymeric composite material where the host polymer, in this case polyimide films, is already formed is a relatively novel concept, especially since the polyimide films maintain their physical and chemical integrity following the modification.

## **B. Results and Discussion**

The two dopants used in this aspect of the study,  $\text{CoCl}_2$  and  $\text{AgNO}_3$ , behaved quite differently under the conditions of the experimentation. It was also discovered that the different natures of the two polyimides used, BTDA-APB and

BTDA-ODA had a profound effect on the resultant types of composite structures formed. The purpose of this Chapter is to outline and explain these differences.

## 1. General film properties

The amount of dopant present initially in the soaking solutions was a much larger amount at all concentrations than would have been present in a film modified by the in-situ approach. If all the dopant dissolved in the solution had penetrated the films, and remained there, the resultant films would probably have been extremely stiff and brittle. As it was, the films were flexible and exhibited very little color change after the soaking.

In both dopant solutions, the BTDA-ODA films "curled" after being soaked. The direction of the "curl" was such that the air side was convex and the glass side had the concave curvature. Thus, the air side was swollen to a greater extent by the diffusing solvent. This disparity then caused the films to curl to relieve the stress.

The BTDA-APB films did not curl when soaked. First of all, the two polyimides were soaked at different temperatures. The BTDA-ODA films were soaked at 100°C. A set of preliminary experiments had previously shown that elevated temperature increased the amount of dopant (AgNO<sub>3</sub>)

able to diffuse into the film.<sup>62</sup> However, when the BTDA-APB films were soaked at that temperature, the films partially dissolved. Thus the decision was made to soak BTDA-APB films at 25°C. At these two different temperatures, both sets of films were soaked at a temperature 180°C below their respective glass transition temperatures.

There was another overriding factor which created rather than removed disparity in the preparation procedure. As was stated in the Chapter III, both films were pre-cured to 200°C before being soaked in the appropriate solutions. The curing accomplishes two purposes: 1) solvent is driven off and 2) imidization takes place. Imidization occurs at different rates and at different temperatures for different polyimides. Thus although both films were cured to 200°C, the BTDA-APB films experienced a much higher degree of cure (imidization) than did BTDA-ODA films. In fact, by virtue of being cured to its  $T_g$ , BTDA-APB films were nearly fully imidized, while BTDA/ODA films underwent virtually no imidization at all.

Direct proof of the extent of imidization was seen in the thermal analysis of the films. Figure 18 is the TGA trace of a BTDA-ODA film soaked in 0.01M  $AgNO_3$  and post cured to 300°C, 20°C above its  $T_g$ . The initial weight loss of 2% was due to residual solvent and surface moisture being lost. There is virtually no mass loss after that point

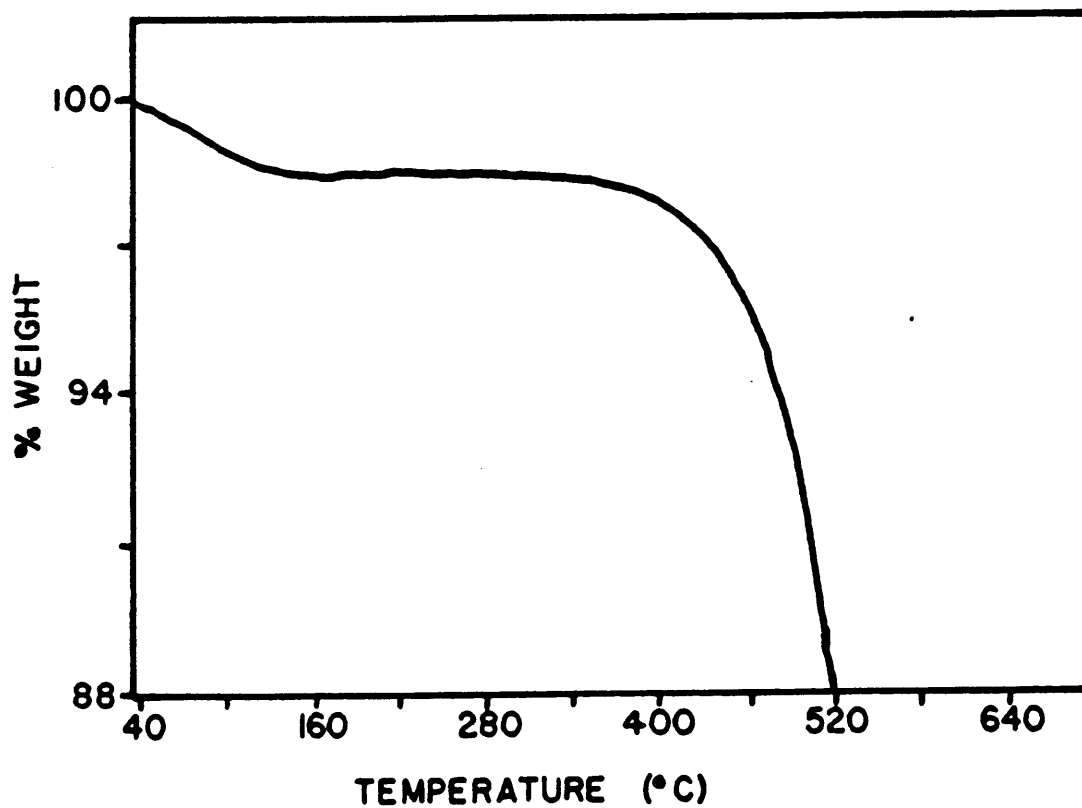


Figure 18. TGA trace of AgNO<sub>3</sub> modified BTDA-ODA film cured through 300°C.

until the film begins to decompose around 500°C. In contrast, Figure 19 is the TGA trace of a similar film cured to only 200°C, in the usual manner. In addition to the typical initial mass loss, there is another 4-5% mass loss from 260° - 300°C. This can be attributed to the loss of water of imidization, which occurs at the glass transition temperature. The  $T_g$  of BTDA-ODA is 285°C. Theoretical calculations show that the mass of water lost through imidization is 5% of the total molecular weight (based on repeat unit mass). Therefore, the BTDA-ODA films which were cured to 200°C, are not fully imidized and subsequently were easily swollen by the soaking solvent.

The BTDA-APB films on the other hand, were imidized with only a 200°C cure. This is borne out by Figure 20 which is the TGA trace of a BTDA-APB film soaked in 0.01 M  $\text{AgNO}_3$  and then cured through 200°C. The significant feature is the lack of any mass loss due to water at the temperature of imidization. This indicates that the film was fully imidized and more solvent resistant than the BTDA-ODA films. To confirm this, pieces of both ODA and APB films were soaked for one hour in neat DMAC at 100°C and 25°C, respectively. The pieces of film were weighed before and after soaking. The BTDA-APB film gained 4% mass upon soaking, while the BTDA-ODA film gained mass of 12% due to solvent uptake.

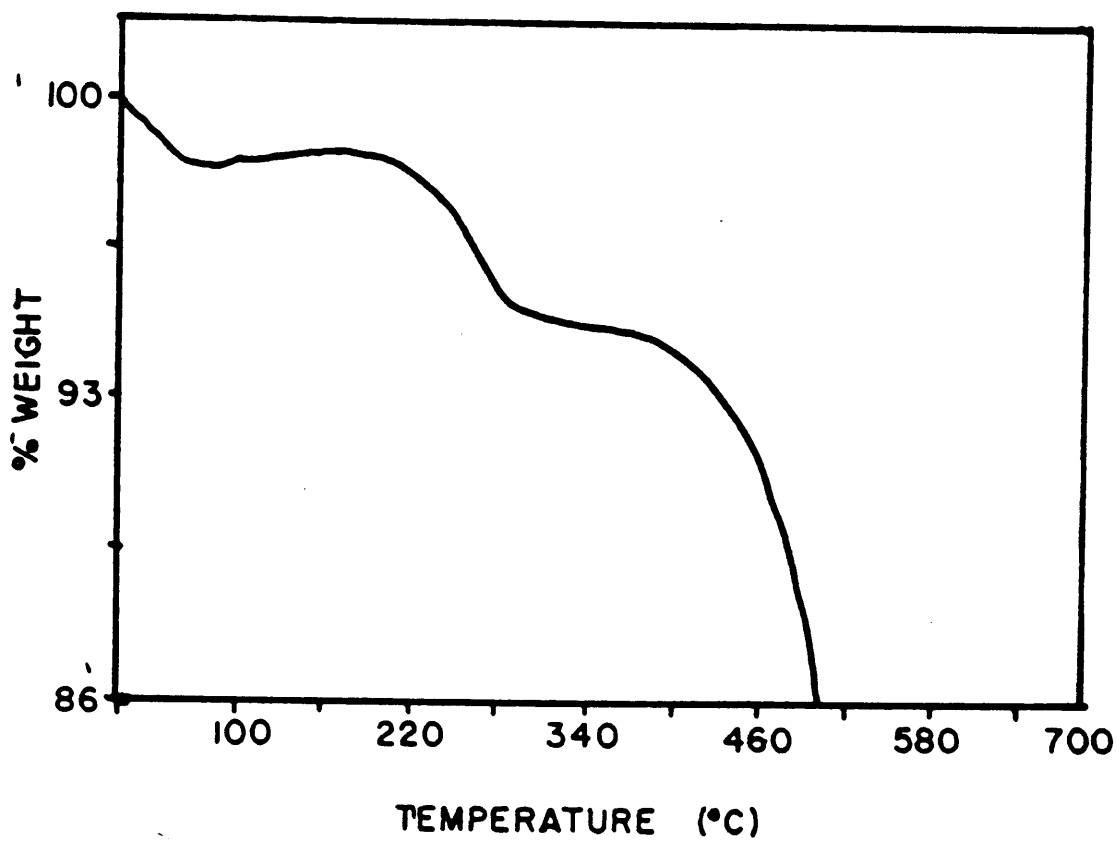


Figure 19. TGA trace of AgNO<sub>3</sub> modified BTDA/ODA film cured through 200°C.

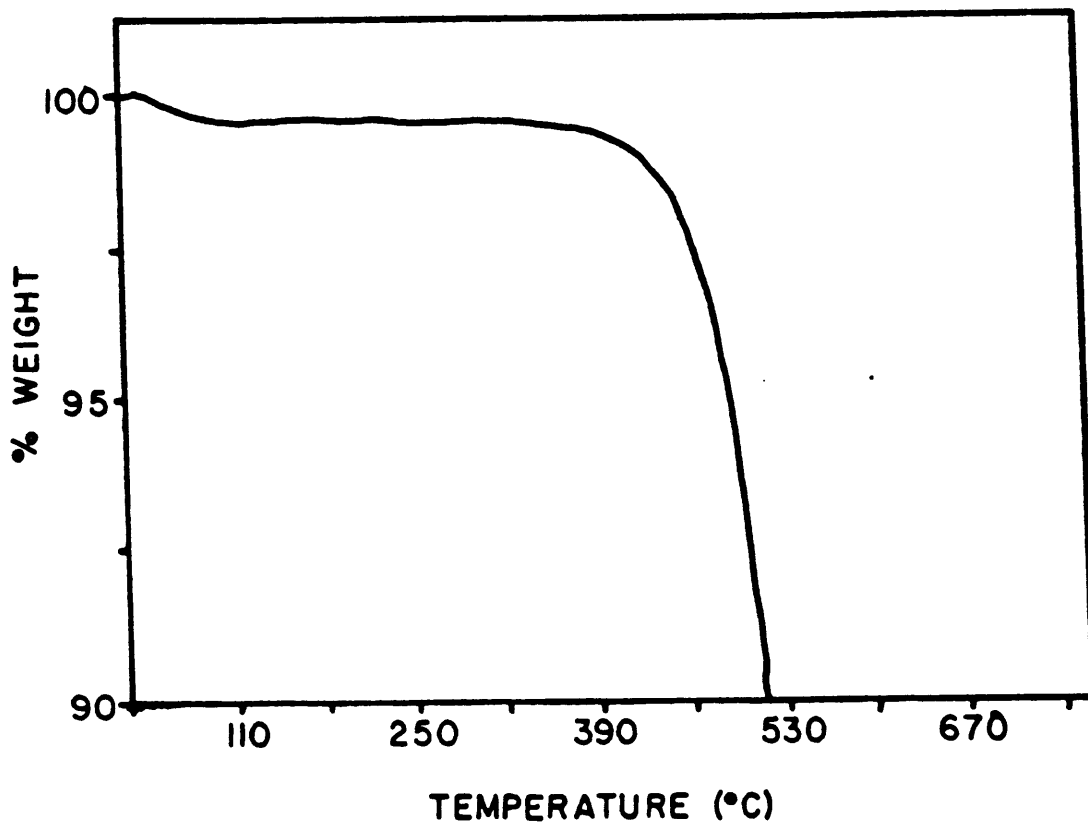


Figure 20. TGA trace of AgNO<sub>3</sub> modified BTDA/APB film cured through 200°C.

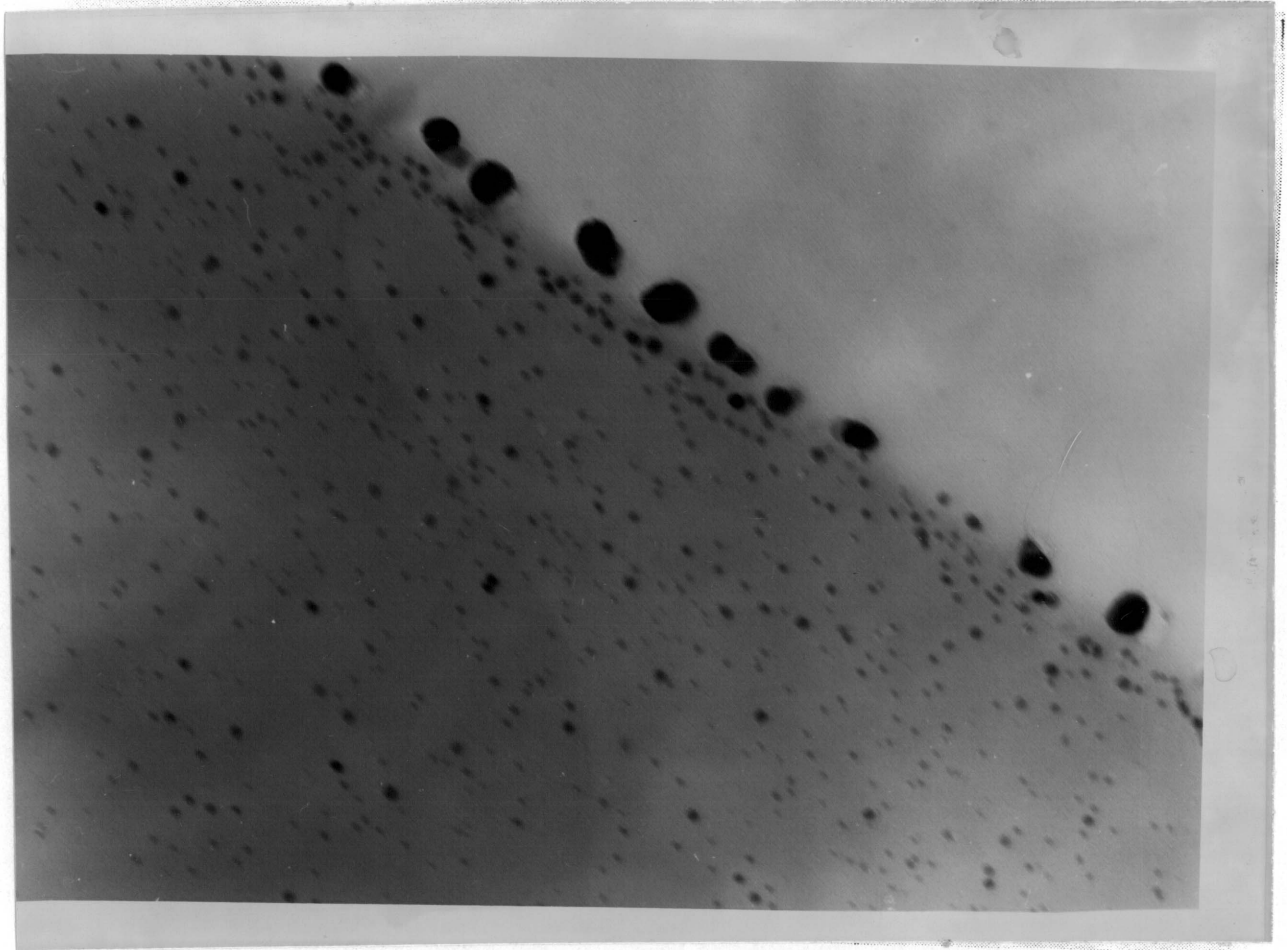
## 2. $\text{AgNO}_3$ as the Dopant

### a. Free-standing films

The principal analysis technique used was TEM. Figures 21 and 22 depict the distribution of dopant material in BTDA-ODA and BTDA-APB, respectively. The difference in the distribution pattern is striking. In both cases, the films had been soaked in 0.10M solutions. The same patterns hold for films soaked at the lower concentrations (0.05M, 0.01M) even though the overall volume of the dopant decreased.

The fact that the BTDA-ODA film shows particles to a greater depth than the BTDA-APB film uphold the theory of the BTDA-ODA films being less imidized. If a BTDA-ODA film is cured to 300°C before soaking, the uptake of dopant is less (Figure 23). Thus it appears that the lack of imidization was a critical factor in allowing the diffusion of the dissolved dopant as well as the nucleation and growth of the dopant species.

The mechanism of particle formation in polyimides is not clearly understood, particularly in the context of infusion deposition. When the films are heated after the soaking, the solvent is driven off and some of the dopant remains behind. It will then either stay ionically

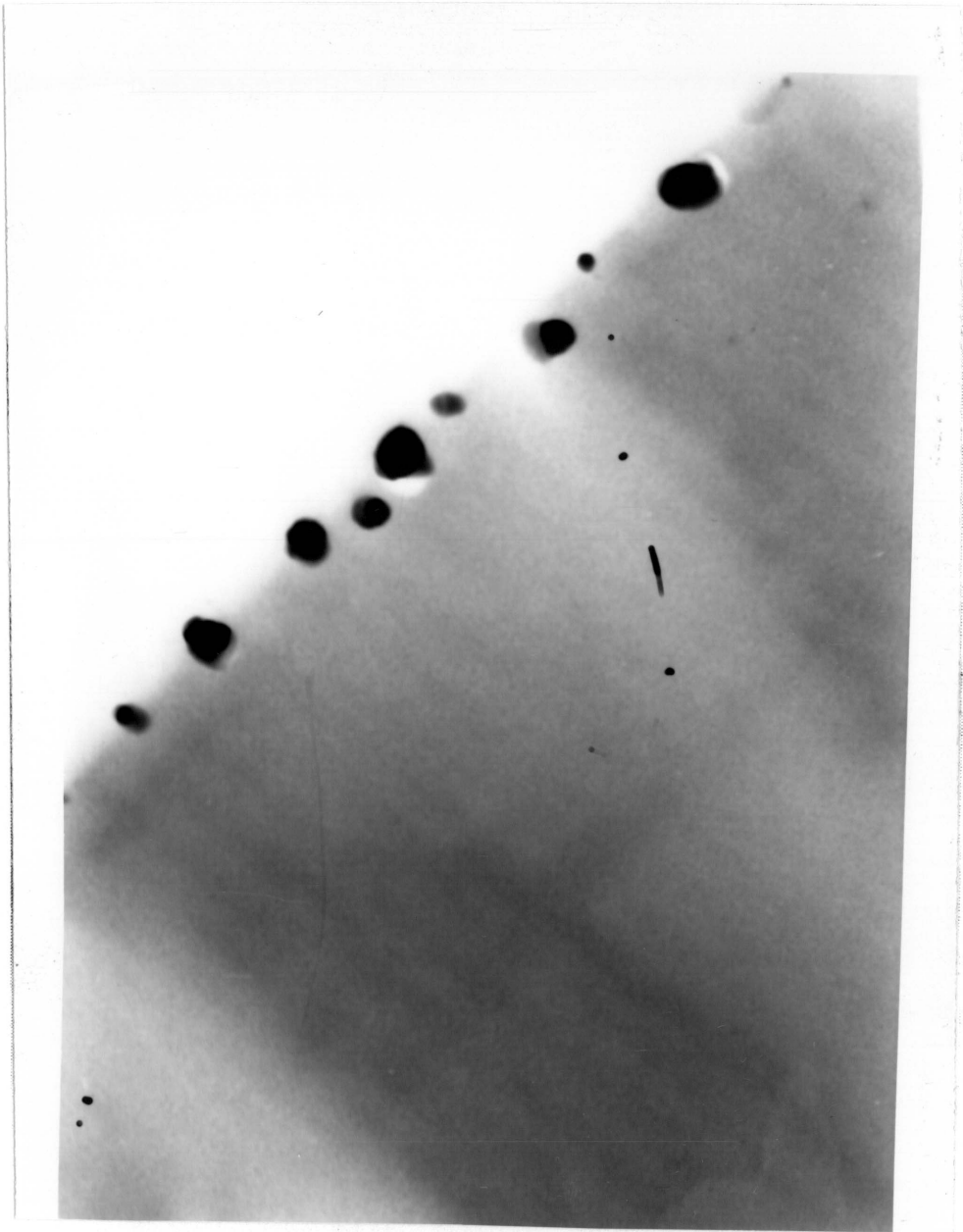


magnification: 120,400X

0.1  $\mu\text{m}$



Figure 21. TEM micrograph of BTDA-ODA film, cured to 200°C, modified with 0.10M AgNO<sub>3</sub> solution at 100°C.



magnification: 120,400X

0.1 um

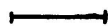
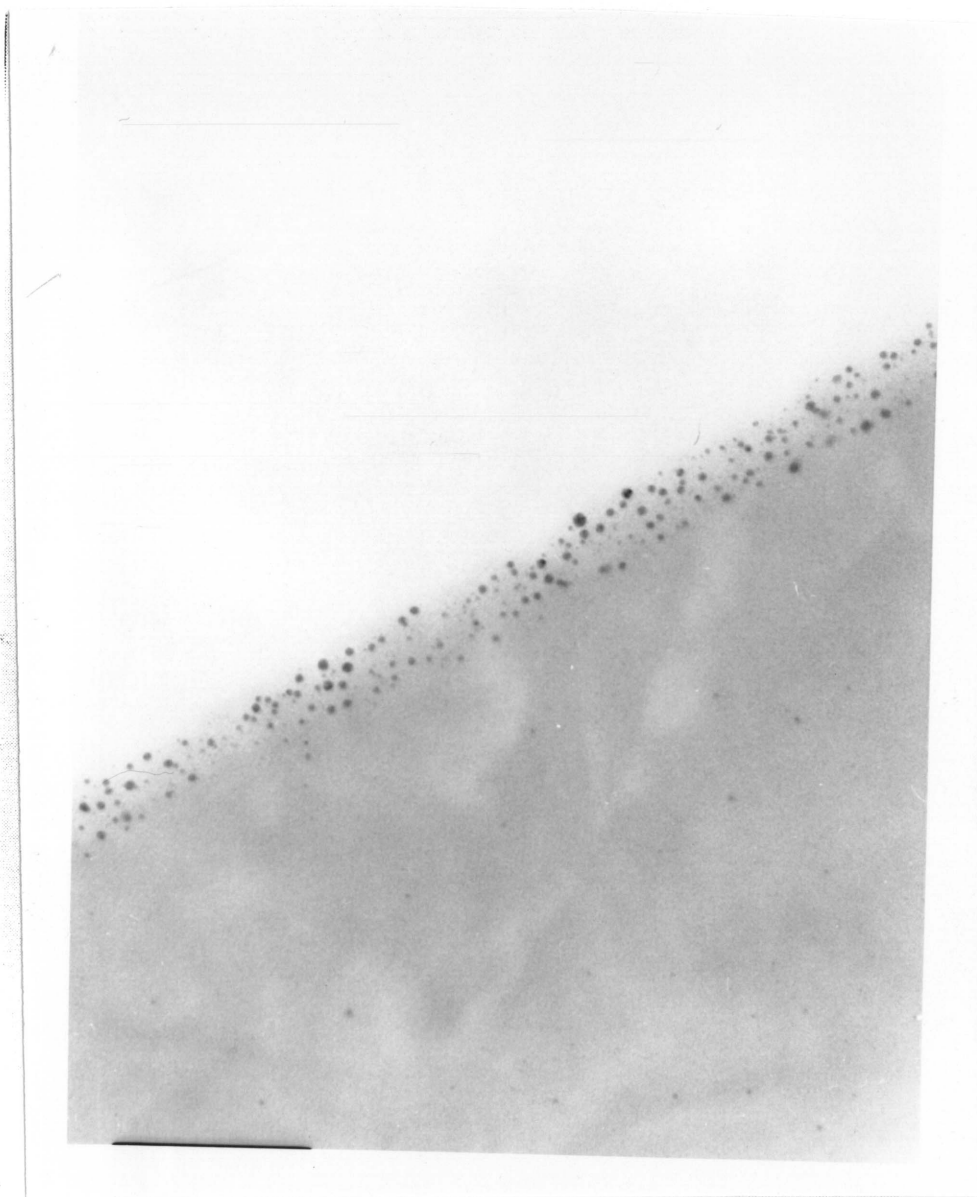


Figure 22. TEM micrograph of BTDA-APB film, cured to 200°C, modified with 0.10M AgNO<sub>3</sub> solution at 25°C.



magnification: 172,000X

0.1 um



Figure 23. TEM micrograph of BTDA-ODA film, cured to 300°C, modified with 0.10 M AgNO<sub>3</sub> at 100°C.

dispersed, coordinated to the polymer, or precipitate as particles and possibly convert to a different chemical form. The fate of the  $\text{AgNO}_3$  in both polyimides appears to be that of a precipitation/nucleation phenomena. It appears that the BTDA-APB films had fewer nucleation sites than did the BTDA-ODA films. Although there were fewer particles in the APB film, they were in general larger than those in the ODA films. Also, bulk elemental analysis revealed that both films had relatively the same amounts of silver present (Table 4). The particle sizes in each film are given in Table 5 and are presented as average measurements. For the ODA films, there were also a few very large particles near the film/air interface. Those particles were generally four times larger than the more uniform particles in the interphase region.

The ODA films do not depict a trend in particle size with dopant concentration even though there was a trend in the overall amount of dopant material in the films. This suggests that there is an intrinsic factor in BTDA-ODA polyimide which allows particles to grow to a limiting size regardless of how much dopant is present. In other words, particle size is a function of the polyimide but not the amount of dopant material initially present. For APB films, there did appear to be a trend of particle size with dopant

**Table 4**

Elemental analysis of AgNO<sub>3</sub> modified films

| <u>polyimide</u> | <u>dopant<br/>concentration</u> | <u>ppm Ag</u> |
|------------------|---------------------------------|---------------|
| BTDA/ODA         | 0.10 M                          | 38            |
| BTDA/ODA         | 0.01 M                          | <1            |
| BTDA/APB         | 0.10 M                          | 33            |
| BTDA/APB         | 0.01 M                          | <1            |

**Table 5**

Particle sizes in AgNO<sub>3</sub> modified films

| <u>polyimide</u> | <u>dopant<br/>concentration</u> | <u>particle size (nm)*</u> |
|------------------|---------------------------------|----------------------------|
| BTDA/ODA         | 0.10 M                          | 11.3                       |
|                  | 0.05 M                          | 11.0                       |
|                  | 0.01 M                          | 16.6                       |
| BTDA/APB         | 0.10 M                          | 46.7                       |
|                  | 0.05 M                          | 40.2                       |
|                  | 0.01 M                          | 13.5                       |

\* measurement does not include the few very large particles present in some films.

concentration. Also, the particles were all virtually the same size.

Regardless of the particle size, analysis by XPS indicated that the surface dopant particles were not  $\text{AgNO}_3$ . As had been anticipated, the dopant had converted during the post-soaking cure time. One of the primary pieces of evidence that the dopant had converted was found in the N 1s narrow scans (Figure 24 and 25). In all films, the only photopeak present was that of the polyimide nitrogen at 400.0 eV. If the dopant had been present as  $\text{AgNO}_3$ , the nitrate nitrogen would have appeared at a binding energy of 405 eV. The nitrate photopeak did not appear at all, even when the film samples were first introduced into the sample chamber of the XPS instrument, indicating that the nitrate ion had not been merely photoreduced during the course of the analysis. The presence of the particles in the films indicates however that the  $\text{Ag}^+$  ion does not remain in a dispersed ionic state.

The silver photopeaks themselves (Figure 26) are not conclusive regarding the nature of the silver dopant. Table 6 lists the Ag 3d binding energies and the atomic percentages for each of the films at different dopant concentrations. Binding energies for  $\text{Ag}^+$  and  $\text{Ag}^0$  differ very little, and the  $3d_{5/2}$  --  $3d_{3/2}$  peak separation is 6.0 eV in both cases.

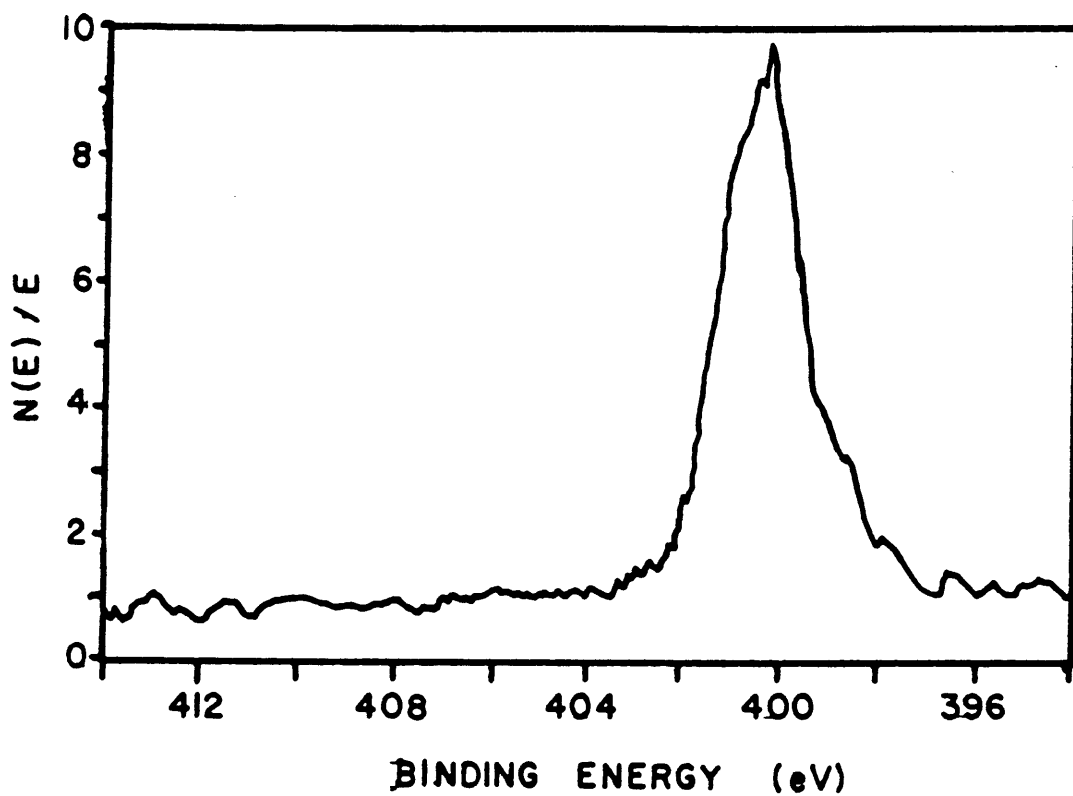


Figure 24. N 1s XPS photopeak from  $AgNO_3$  modified BTDA-ODA.

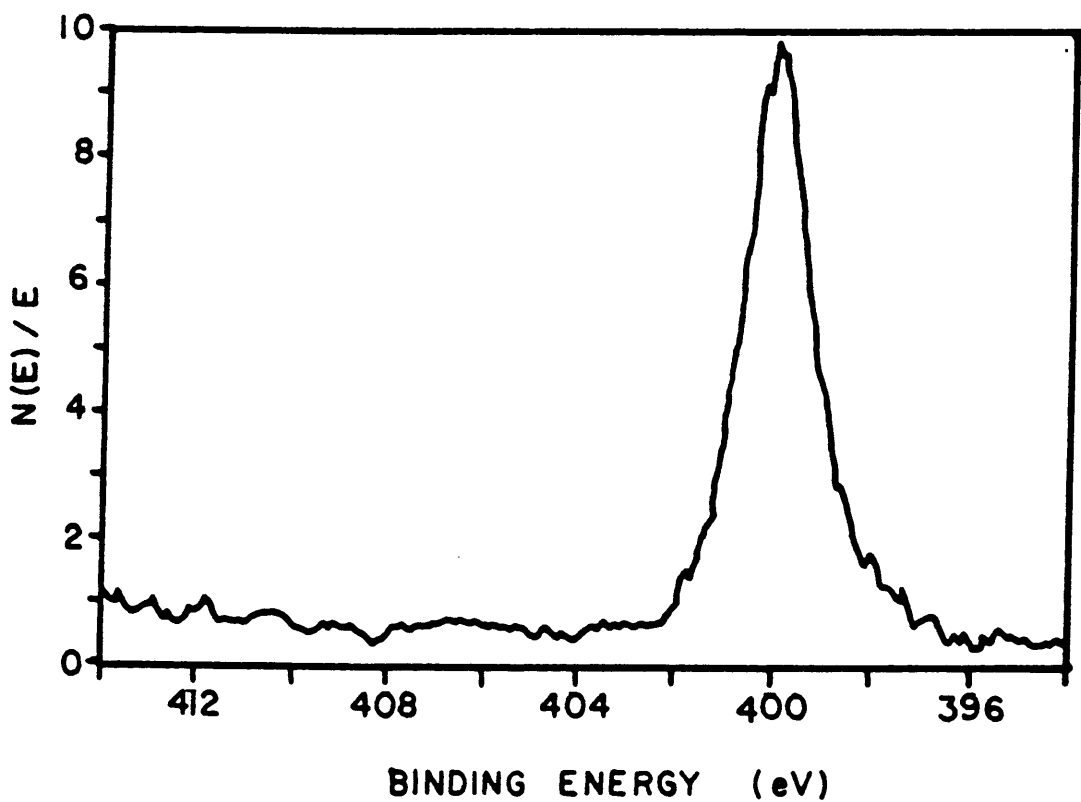


Figure 25. N 1s XPS photopeak from  $\text{AgNO}_3$  modified BTDA-APB.

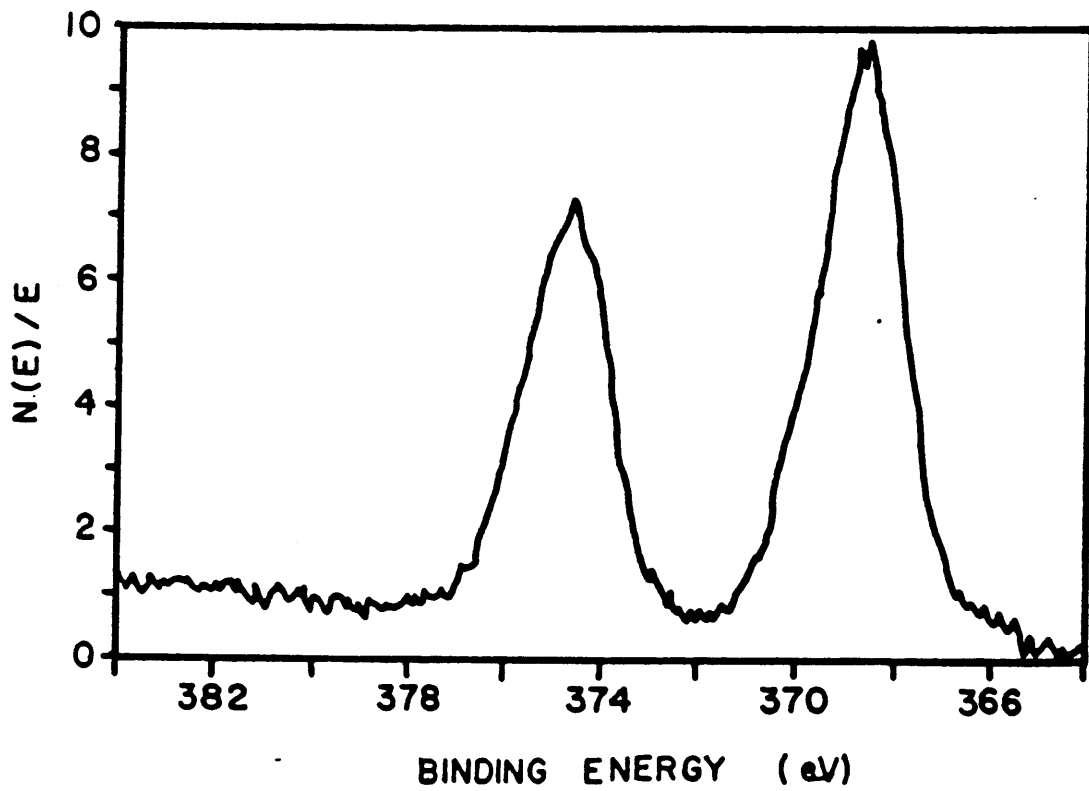


Figure 26. Ag 3d(3/2,5/2) XPS photopeaks.

**Table 6**

Ag 3d binding energies and surface atomic percentages

| <u>polyimide</u> | dopant<br>concentration | binding energy (eV)        |                            | surface<br>atomic % |
|------------------|-------------------------|----------------------------|----------------------------|---------------------|
|                  |                         | <u>Ag 3d<sub>3/2</sub></u> | <u>Ag 3d<sub>5/2</sub></u> |                     |
| BTDA/ODA         | 0.10 M                  | 374.1                      | 368.1                      | 2.3                 |
|                  | 0.05 M                  | 374.0                      | 368.0                      | 2.6                 |
|                  | 0.01 M                  | 374.0                      | 368.0                      | 1.2                 |
| BTDA/APB         | 0.10 M                  | 373.9                      | 367.9                      | 2.7                 |
|                  | 0.05 M                  | 374.0                      | 368.0                      | 0.7                 |
|                  | 0.01 M                  | 374.0                      | 367.9                      | 0.22                |

For identification of silver compounds it is helpful to examine the Auger peaks that also appear when a silver sample is irradiated by an X-ray source. If a vacant orbital is present in a core electron level, there can be a transition of an electron from a higher level to the lower level in order to stabilize the ion. In the process energy is released, causing an electron to be emitted with a characteristic kinetic energy. This is the Auger process. Chemical shifts due to change in oxidation state of a specie are often more pronounced in the Auger process than XPS binding energies, particularly in transition metals.<sup>63</sup> To examine the the Auger parameter of the silver present on the film surface, a silver metal standard was analyzed by XPS. The Auger peaks observed in the scan were compared with those seen in the wide scan of a modified film.

The Auger parameter ( $\alpha$ ) is calculated by the following equation:

$$\alpha = K.E.\text{Auger electron} + B.E.\text{XPS electron} \quad (11)$$

The kinetic energy of the Auger electron is determined by subtracting the binding energy of the Auger transition in the XPS spectra from the energy of the X-Ray source. In this case the source was the MgK line at an energy of 1253.6 eV. For the silver metal standard, the XPS binding energy

was 368.1 eV, and the Auger kinetic energy was determined to be 358.7 eV. Thus the Auger parameter is calculated to be:

$$\alpha_{\text{Ag metal}} = 358.7 \text{ eV} + 368.1 \text{ eV} = \underline{726.8 \text{ eV}} \quad (12)$$

For the AgNO<sub>3</sub> modified film sample measured, the XPS binding energy was 367.9 eV and the Auger kinetic energy was determined to be 356.3 eV, thus;

$$\alpha_{\text{Ag modified film}} = 356.3 \text{ eV} + 367.9 \text{ eV} = \underline{724.2 \text{ eV}} \quad (13)$$

The difference of 2.6 eV is significant. The Handbook of X-ray Photoelectron Spectroscopy published by Perkin-Elmer contains charts which cross-reference the Auger parameter with the XPS binding energies.<sup>64</sup> Given the data mentioned above, the chart for silver indicated that silver was present as Ag<sup>+1</sup>, most likely as Ag<sub>2</sub>O.

According to Cotton and Hart,<sup>65</sup> Ag<sub>2</sub>O can be formed through the action of base on silver nitrate. The dark brown oxide precipitate then decomposes above 160°C to give silver metal and oxygen. The films analyzed here had been cured to 200°C after being modified. Thus, if the silver nitrate in the films had converted to silver oxide, it would have in turn reduced to silver metal. The Auger parameter, however, indicated that the silver was present as Ag<sup>+</sup>. Even

though  $\text{Ag}_2\text{O}$  is said to decompose above  $160^\circ\text{C}$ , the extreme small size of the particles and the high heat capacity may have caused an increase in the temperature at which the particles would decompose.

Confirming evidence for the presence of  $\text{Ag}_2\text{O}$  would have been the presence of an oxide oxygen photopeak. In none of the modified film samples however did a distinct oxide oxygen photopeak appear. It may have been obscured by the imide oxygen photopeak. However, the amount of oxygen contributed by silver oxide was expected to be minimal at best (0.5 - 1.0 atomic percent) in these films. Curve resolution of the oxygen peak from a modified film did not reveal an oxide oxygen peak.

The presence of dopant particles in the films did not affect the thermal properties. Table 7 summarizes the  $T_g$  and PDT data for both polyimides. The promising aspect of the data is that although there is a microcomposite structure near the film surface, the bulk thermal properties did not change. Thus it becomes possible to modify the interface of a film without affecting the desirable bulk properties, particularly thermal stability.

**Table 7**Thermal data from AgNO<sub>3</sub> modified films

| <u>polyimide</u> | <u>dopant<br/>concentration</u> | <u>T<sub>g</sub> (°C)</u> | <u>PDT (°C)</u> |
|------------------|---------------------------------|---------------------------|-----------------|
| BTDA/ODA         | 0.10 M                          | 279                       | 524             |
|                  | 0.05 M                          | 282                       | 529             |
|                  | 0.01 M                          | 279                       | 535             |
|                  | none                            | 284                       | 525             |
| BTDA/APB         | 0.10 M                          | 198                       | 543             |
|                  | 0.05 M                          | 194                       | 524             |
|                  | 0.01 M                          | 198                       | 538             |
|                  | none                            | 198                       | 535             |

## b. Simulated bonds

For recall purposes, simulated bonds were prepared by sandwiching two modified films around a nonmodified film and "bonding" the whole assembly. The tri-layer samples generally consolidated into one fused film. In all cases, the samples were a darker color after "bonding" than before, but they were still relatively translucent. The bonded films were much more rigid than the individual films.

Figure 28 depicts the particle distribution pattern in a BTDA/ODA bonded specimen. The outstanding feature is the depletion zone. The depletion zone is defined as the area in the film between the single line of particles at the interface and the rest of the particles. Figure 21 showed the same film before bonding where there was no such zone.

In addition, the particles are three to four times larger in the "bonded" film than in the free-standing films. Table 8 lists the particle sizes. The particle sizes in the pre-bonded films are included for comparison. Two different mechanisms are proposed for the enhancement in size. Either the particles are merely coalescing to form larger particles, or the larger particles are getting larger at the expense of the smaller particles. From the pictures available, it appears that it is a combination of both mechanisms. We believe that if the simulated bonds had been held at the final temperature of 300°C for a longer time,



magnification: 43,400X

0.5  $\mu\text{m}$



\* arrows indicate interface between modified film (below) and nonmodified film (above)

Figure 27. TEM micrograph depicting the particle distribution in the "simulated bond" using  $\text{AgNO}_3$  modified BTDA-ODA films.

**Table 8**

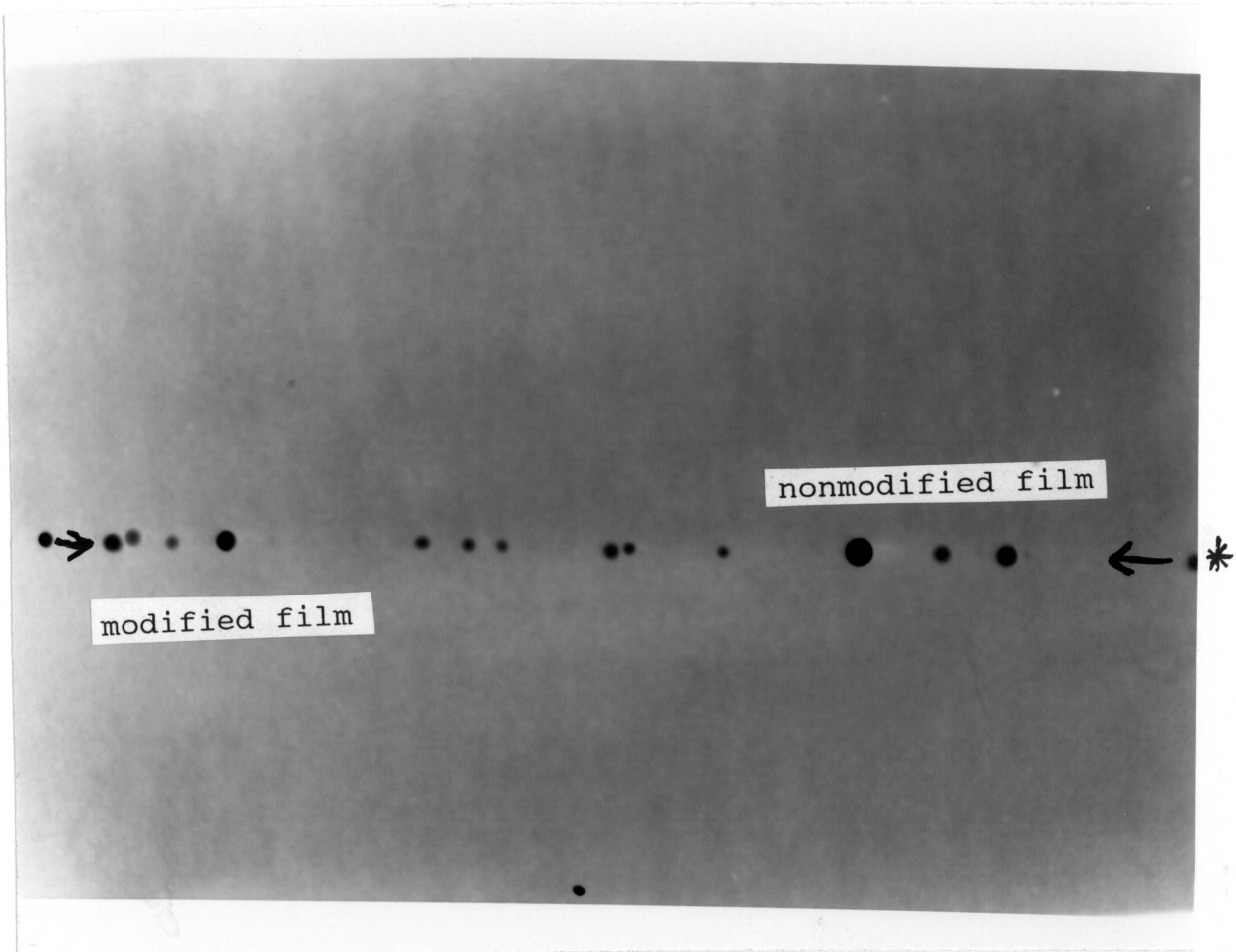
Particle sizes in simulated bonds. Particle sizes in pre-bond films are included for reference.

| polyimide | dopant concentration | particle size (nm) |                |
|-----------|----------------------|--------------------|----------------|
|           |                      | after bonding      | before bonding |
| BTDA/ODA  | 0.10 M               | 30                 | 11             |
|           | 0.05 M               | 20                 | 11             |
|           | 0.01 M               | 25                 | 17             |
| BTDA/APB  | 0.10 M               | 27                 | 47             |
|           | 0.05 M               | 11                 | 40             |
|           | 0.01 M               | 12                 | 14             |

the depletion zone would be larger and the particle sizes would be larger. In other words, the growth of the dopant particles is time and temperature dependent.

The mobility of the dopant material in the BTDA-ODA matrix is not a clearly understood process. At such small particle sizes, gravity appears not to be a major factor. The nature of the dopant material is more of an influence. Given that the dopant had converted to  $\text{Ag}_2\text{O}$  (decomposes above  $160^\circ\text{C}$ ) and possibly  $\text{Ag}^0$  (m.p. =  $961^\circ\text{C}$ ), the particles would not grow through melting and coalescing. There would need to be a distinct process of particles breaking down and reforming, atom by atom, or perhaps dissolving in the polyimide and reprecipitating.

With BTDA-APB bonded specimens there was no significant change in the particle distribution. The line of particles in Figure 28 indicates the interface between the modified film and nonmodified film in the bond. While there was no apparent change in the distribution, the size of the particles actually decreased. Again, the theory of the fully imidized BTDA-APB is invoked to explain that phenomena. Since the film was imidized from the beginning of the infusion process, the movement of particles at any time would be severely limited.



magnification: 120,400X

0.1 um



\* arrows indicate interface between modified film (below) and nonmodified film (above)

Figure 28. TEM micrograph depicting the particle distribution in the "simulated bonds" using  $\text{AgNO}_3$  modified BTDA-APB.

### 3. $\text{CoCl}_2$ as the Dopant

#### a. Free-standing films

Particles did not form in BTDA-ODA and BTDA-APB films which had been soaked in  $\text{CoCl}_2$  solutions and cured to  $200^\circ\text{C}$ . The dopant appeared to remain ionically dispersed throughout the polyimide matrix. There was ample evidence that cobalt chloride was present in the films. Table 9 lists the results of bulk elemental analysis of both films, prepared from solutions containing high and low concentrations of dopant. Unlike the silver modified films, there is not a trend between amount of dopant present and the dopant concentration. There even appears to be more cobalt present in the BTDA-ODA film which was soaked in the lower concentration solution. It must be kept in mind though, that at so small a measurement, a difference of 0.005% is well within measurement error.

Another piece of anomalous data is the inordinately large amounts of chlorine present relative to the amounts of cobalt present. Chlorine is easily introduced as a contaminant. Even though extreme care was taken to handle the film specimens with tweezers, an inadvertant fingerprint would deposit some chlorine.

Analysis by XPS revealed very little cobalt on the surface of the films, relative to the amount that was in the

**Table 9**

Elemental analysis of  $\text{CoCl}_2$  modified films

| <u>polyimide</u> | <u>dopant<br/>concentration</u> | <u>% Co</u> | <u>% Cl</u> |
|------------------|---------------------------------|-------------|-------------|
| BTDA/ODA         | 0.10 M                          | 0.013       | 0.24        |
|                  | 0.01 M                          | 0.018       | 0.17        |
| BTDA/APB         | 0.10 M                          | 0.033       | 0.19        |
|                  | 0.01 M                          | 0.018       | 0.17        |

bulk. The Co 2p signal (Figure 29) was weak and largely obscured by noise as well as the oxygen Auger peaks that are present in the same energy range (800 - 780 eV). The lack of an O 1s oxide peak (Figure 30) indicated that the dopant had apparently not converted, but had remained ionically dispersed in the film.

Thermal analysis of these films revealed that the presence of the dopant had little effect on the thermal properties of BTDA-ODA and BTDA-APB polyimide films. The values obtained for the glass transition temperatures and the polymer decomposition temperatures were virtually identical to those listed in Table 7 for the AgNO<sub>3</sub> modified films. This would indicate that if the dopant is ionically dispersed in the polyimide matrix, it is not coordinated to a great extent to the polymer. If coordination had taken place, the molecular flexibility of the film would decrease. This would in turn lead to a higher glass transition temperature and most likely a lower polymer decomposition temperature.

#### b. Simulated bonds

The effects of pressure and temperature were not enough to bring about precipitation, nucleation and growth of the dopant material. TEM analysis of the simulated bonds did not reveal any particulate matter in the films, much less at the

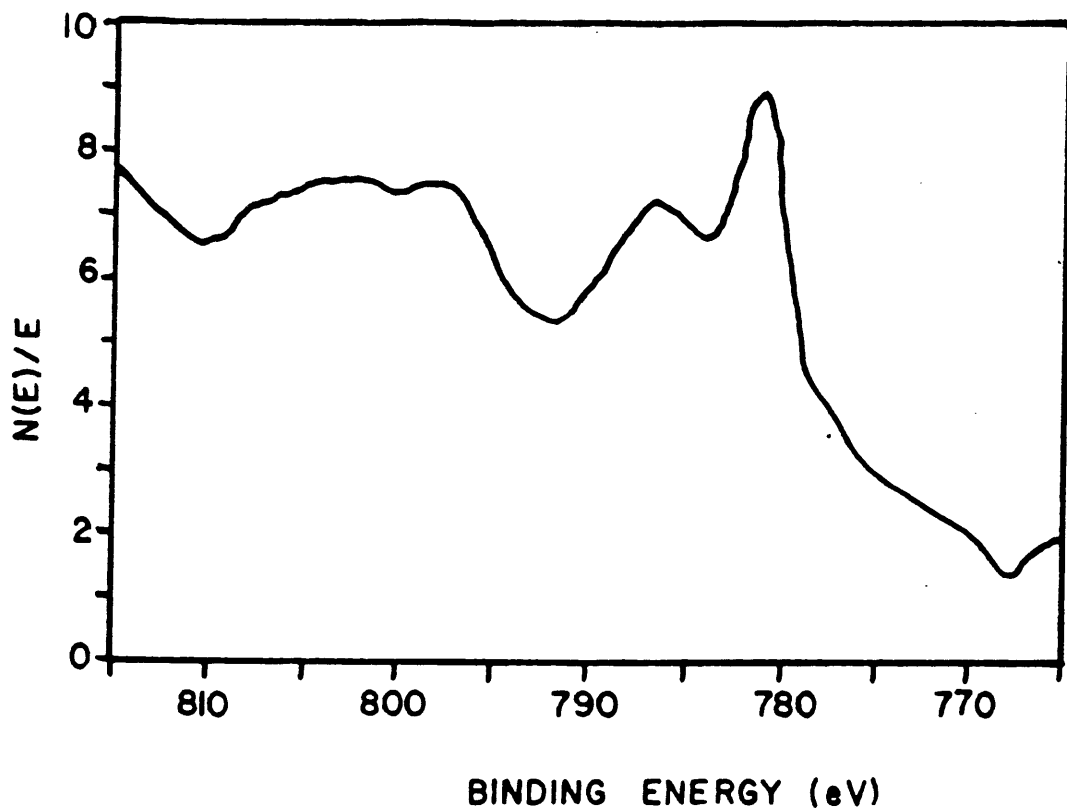


Figure 29. Co 2p<sub>(1/2,3/2)</sub> XPS photopeaks from BTDA-APB film modified with 0.10 M CoCl<sub>2</sub> solution.

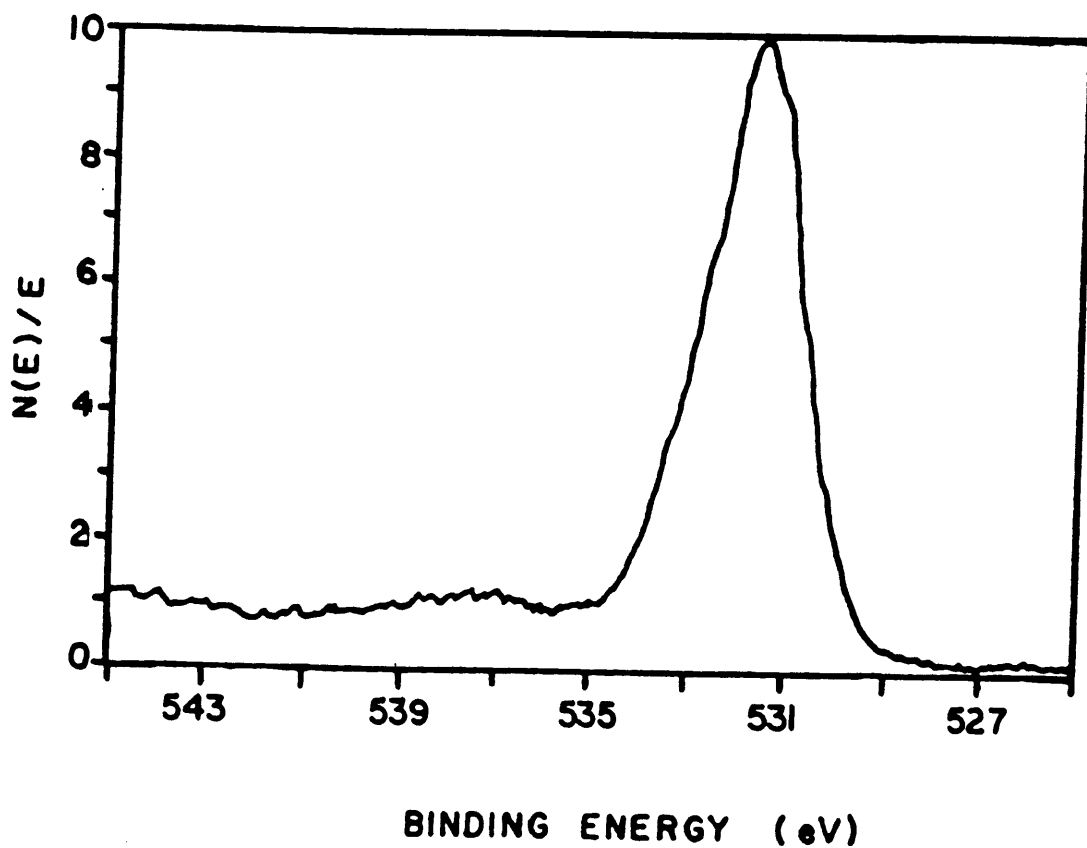


Figure 30. O 1s XPS photopeak from BTDA-APB film modified with 0.10 M  $\text{CoCl}_2$  solution.

film interfaces. This stands in contrast to the results of the in-situ study of Chapter 4, where cobalt doped films which were cured to 300°C under pressure (no air surface) did reveal dopant particles in the bulk of the films. The three layers of film in the simulated bond fused together during the bonding, indicating that there were not surface layers of  $\text{CoCl}_2$  that could have prevented bonding. The obvious conclusion is that the dopant is ionically dispersed and the nature of the dispersion is such that extreme conditions would be required to overcome the dispersion forces and precipitate the dopant.

## Chapter VI

### Conclusions

Two different approaches were used toward the objective of preparing polyimide/metal gradient microcomposite films. The first approach, termed "in-situ chemical generation," yielded results that were less than hopeful, but still shed valuable light on the nature of microcomposite adhesives. The second approach, termed, "infusion deposition," was designed to insure the presence of a concentration gradient at the film surface, and to observe it directly.

#### **A. In-situ Chemical Generation of Dopant**

Under the conditions employed, this technique is not appropriate for preparing modified polyimides which have enhanced adhesive properties. The dopant migrates to the interfaces to form a weak boundary layer. Cobalt(II) chloride was an easier dopant to study in this context since it has different XPS binding energies than the metal of the adherends (Al) employed. While  $\text{Al}(\text{acac})_3$  was shown to affect the thermal properties of BTDA/APB, and it did undergo conversion to the oxide form as was desired; the end result was that it did not improve adhesion and it did not lead to a gradient microcomposite structure. Attempts to

use solid  $\text{AlO}(\text{OH})$  as a dopant proved unsuccessful because the low surface energy of the particles caused aggregation.

Bond-line studies revealed that under bonding conditions  $\text{CoCl}_2$  does not form a gradient structure in the polyimide films.

### **B. Infusion Deposition of Dopant**

This technique has been shown to produce distinct, near surface gradient microcomposite structures in BTDA/ODA films using  $\text{AgNO}_3$  as the dopant. BTDA/APB polyimide films did not yield a gradient structure, due largely to the high extent of imidization in BTDA/APB at  $200^\circ\text{C}$ .

When these films were put in a simulated bond, there was evidence of redistribution of the microcomposite structures. Choosing the right polyimide and the right dopant are crucial factors in developing a final gradient microcomposite structure in thin films.

The overall thermal properties of the infusion deposition modified films did not change. The local polymer around the particles may have been affected, but the extent of film modification was so low (<5% by volume) that the bulk properties did not change. The encouraging aspect is that in an adhesive bond, the bulk adhesive would retain the original thermal properties, while the modified interphases would take on different thermal and physical properties,

arising from polymer/particle interactions. In other words, a property defined gradient would be established.

### **C. Future Work**

Based on the results of this present study, infusion deposition is a valid modification technique which can be refined to yield even greater control over extent and location of microcomposite structures in polymer films. Toward that end, the following are suggested as crucial areas of study:

- finding the right combination of polyimide (or other polymer) and dopant that will yield a stable microcomposite material.
  
- develop techniques which can ascertain the physical properties of the microcomposite zone of the modified polymers.
  
- develop appropriate methods for accurately testing the adhesive properties of films with known gradient microcomposite structures.

## VII - References

### Introduction

1. R.P. Sheldon, Composite Polymeric Materials (Applied Science Publishers, New York, 1982).
2. W.M. Edwards and I.M. Robinson, U.S. Patent No. 2,710,853 (1955).
3. A.L. Endrey, Canadian Patent No. 659,328 (1963).
4. R.G. Spain and W.C. Tincher in, Reinforced Phenolic, Polyester, Polyimide and Polystyrene Systems, Carlos Hilado, ed., Technomic Publishing Co., New York, 116-127 (1974).
5. A.K. St.Clair and L.T. Taylor, J. Macromol. Sci.-Chem **16** 95 (1981).
6. J.C. Anderson, U.S. Patent No. 4,109,052 (1978).
7. R.H. Bott, Characterization of Modified Polyimide Adhesives, Ph.D Dissertation, Virginia Polytechnic Institute and State University, (1988).
8. B. Madigan, Employment of Metal-modified Polyimide to Achieve Optimum Conductance at an Aluminum Joint, M.S. thesis, Virginia Polytechnic Institute and State University (1983).
9. S. Numata, K. Fujisaki, D. Makino and N. Kinjo in Recent Advances in Polyimide Science and Technology, W.D. Weber and M.R. Gupta, eds. (SPE, 1987).
10. Handbook of Chemistry and Physics, 62nd edition, CRC Press, Boca Ratan, FL D-162 (1982).

### Literature Review

11. W.B. Hillig, "Composite Materials," Kirk-Othmer Encyclopedia of Chemical Technology, 3rd edition, vol.6, John Wiley & Sons, New York 683 (1979).
12. A. Kelly, "Composite Materials: an Overview," Encyclopedia of Materials Science and Engineering, vol. 1 Pergamon Press, Oxford, Eng. 757 (1986).

13. W.V. Titow and B.J. Lanham, Reinforced Thermoplastics (Halstead Press, New York 1975).
14. Fillers and Reinforcements for Plastics, Advances in Chemistry Series, no. 134; R.D. Deanin and N.R. Schott, eds. (ACS, Washington, D.C. 1974).
15. Delmonte, J. in Metal-Filled Polymers, S.K. Battacharya ed., Marcel Dekker, Inc, New York 143-164 (1986).
16. M. Ratzsch, H.-J. Jacobastch, and K.-H. Freilag in Polymer Composites, B. Sedlack, ed., Walter de Gruyter & Co., Berlin, GDR 413-430 (1986).
17. Y.G. Lin, J.P. Pascault and B. Sautereau in Polymer Composites, B. Sedlack, ed., Walter de Gruyter & Co., Berlin, GDR 373-380 (1986).
18. G. Challa, A.J. Schouten, G. ten Brinke and H.C. Meinders in Modification of Polymers, ACS Symposium Series 121, C.E. Carraher Jr. and M. Tsuda, eds., ACS, Washington D.C. 7-22 (1980).
19. M.D. Rausch et.al. in Metal-Containing Polymeric Systems, J.E. Sheats, C.E. Carraher Jr. and C.U. Pittman, Eds., Plenum Press, New York 43 (1985).
20. S. Ohnishi, Presentation at the 1987 International meeting of the Adhesion Society, Williamsburg, VA.
21. B. Kovar, Materials Edge, no. 3, 7 (1988).
22. S. Mazur, U.S. Patent No. 4,512,855 1985.
23. S. Mazur and S. Reich, J. Phys. Chem. **90** 1365 (1986).
24. R.J. Angelo, U.S. Patent No. 3,073,785 1963.
25. A.J. Endrey, U.S. Patent No. 3,073,784 1963.
26. E. Kohr and L.T. Taylor, Macromolecules **15**, 379 (1982).
27. T.L. Wohlford, J. Schaaf, L.T. Taylor, T.A. Furtsch, E. Kohr and A.K. St.Clair in Conductive Polymers, R.B. Seymour, ed., Plenum Press, New York 7-22 (1981).
28. J.D. Rancourt, G.M. Porta and L.T. Taylor, Thin Solid Films **158**, 189 (1988).

29. S. Ezzell, Modification of Polyimide Films Via Tin Complex Formation, M.S. thesis, Virginia Polytechnic Institute and State University, 1983.
30. R.K. Boggess and L.T. Taylor in Polyimides, 2nd Annual Ellenville Polyimide Conference, K.L. Mittal ed. (Plenum Press, NY 1986).
31. G.M. Porta, Metal-Polymer Interactions, Ph.D Dissertation, Virginia Polytechnic Institute and State University, 1989.
32. M.N. Sarboluki, NASA Technical Brief, 3 item 36 (1978).
33. L. Holliday and J. Robinson, J. Mat. Sci., **8**, 301 (1973).
34. R.S. Raghava, Polymer Composites **9**, 1 (1988).
35. D.M. Bigg, Polymer Composites **8**, 115 (1987).
36. L. Aras, R.P. Sheldon and H.M. Lai, J. Polym. Sci.: Polym. Letters **16**, 27 (1985).
37. R. Singh and R.W. Roberts, Polymer Composites **6**, 58 (1985).
38. R.P. Kusey in Metal-Filled Polymers, S. Bhattacharya, ed., Marcel-Dekker, Inc., New York 66-82 (1986).
39. H. Ziebland, Reinforced Plastics, 25 April 1981.
40. R.C. Progelhof, J.L. Throne and R.R. Ruetsch, Polym. Eng. Sci. **16**, 615 (1976).
41. D.V. Duchane, J. Vac. Sci. Technol. **18**, 1183 (1981).
42. D.A. Wrobleski, D.L. Cash, D.V. Duchane and B.E. Lehnert, Poly. Mat. Sci. Eng. **57**, 164 (1987).
43. J.D. Rancourt and L.T. Taylor, Final Project Report to Travenol Laboratories and Clemson University; Virginia Polytechnic Institute and State University, 1989.
44. H.L. Frisch in Non-Equilibrium Thermodynamics Variational Techniques and Stability, R.J. Donnelly, R. Herman and I. Prigogine, Eds., University of Chicago, Chicago, IL 277-280 (1965).

45. D.S. Cohen, J. Poly. Sci.: Poly. Phys. Ed. **21**, 2057 (1983).
46. J. Crank and G.S. Park in Diffusion in Polymers, J. Crank and G.S. Park, Eds., Academic Press, Inc., London 1-7 (1968).
47. G.S. Park, in Diffusion in Polymers, J. Crank and G.S. Park, Eds., Academic Press, Inc. London 141-145 (1968).
48. R.J. Kokes, F.A. Long and L.J. Hoard, J. Chem. Phys. **20** 1711 (1952).
49. F.A. Long and D. Richman, J. Am. Chem. Soc. **82**, 513 1960.
50. H.L. Frisch, T.T. Wang and T.K. Kwei, J. Poly. Sci.:A-2 **7**, 879 (1969).
51. R.G. Carbonell, G.C. Sarti, C. Gostoli and J. Riccoli, J. Appl. Polym. Sci. **32**, 3627 (1986).
52. R.H. Peters in Diffusion in Polymers, J. Crank and S.J. Park, Eds. (Academic Press, Inc., London 1968).

### Experimental

53. L.S. Smith, Study of A Microcomposite Metal-Doped Polyimide Ashesive, M.S. thesis, Virginia Polytechnic Institute and State University, 1989.

### In-Situ Chemical Generation

54. F.D. Lemkey, "In-Situ Composites," Encyclopedia of Materials Science and Engineering vol. 3, Pergamon Press, Oxford, Eng. 2267 (1986).
55. D.G. Madeleine, A Study of Polyimide Films Modified With Gold, Ph.D Dissertation, Virginia Polytechnic Institute and State University, 1988.
56. J.D. Rancourt, R.K. Boggess, L.S. Horning and L.T. Taylor, J. Electrochem. Soc. **134**, 85 (1987).
57. J.D. Rancourt and L.T. Taylor, *Macromolecules* **20**, 790 (1987).

58. R.K. Boggess and L.T. Taylor, *J. Polym. Sci.: Part A, Polym. Chem.* **25**, 685 (1987).
59. J.D. Rancourt, Cobalt Modified Polyimides, Ph.D. Dissertation, Virginia Polytechnic Institute and State University, 1987.
60. J.D. Rancourt, R.K. Boggess and L.T. Taylor, *Polym. Mater. Sci. Eng.* **53**, 74 (1985).
61. J.D. Rancourt, L.S. Horning and L.T. Taylor, *Polym. Mater. Sci. Eng.* **56**, 670 (1987).

#### Infusion Deposition

62. M.M. Bilbirnie and J.D. Rancourt, Undergraduate Research Report, Virginia Polytechnic Institute and State University, 1989.
63. G. Wilson, VPI & SU, personal communication.
64. Handbook of X-Ray Photoelectron Spectroscopy, C.D. Wagner, W.M. Riggs, L.E. Davis, J.F. Moulder and G.E. Muilenberg, eds., Perkin-Elmer Corporation, Physical Electronics Division, 6509 Flying Cloud Dr., Eden Prarie, MN, 55344.
65. S.A. Cotton and F.A. Hart, The Heavy Transition Elements, MacMillan Press LTD., New York 138-139 (1975).

## VITA

Leslie Sauder Horning was born February 2, 1964 in Ephrata PA, to Reuben and Sarah Horning. In June of 1982 he graduated with honors from Ephrata Area Senior High School. He received a National Merit Scholarship and began attending Eastern Mennonite College in September of 1982. While an undergraduate, he spent two summers (1985, 1986) working as a research assistant in the laboratories in the laboratories of Dr. Larry Taylor at Virginia Tech. He graduated from EMC in May of 1986 with a B.S. in Chemistry/Biology.

Graduate studies were delayed for a year and a half in which time he married Crystal Driver on January 3, 1987, and worked as a chemistry lab instructor at Eastern Mennonite College. He also had a part time job as a carpenter during that time. After his wife Crystal received an M.S. degree in Community Counseling from Shippensburg University, PA, they moved to Blacksburg in December of 1987 and Les began his graduate program, working with Dr. Larry T. Taylor.

While completing degree requirements, Les became a member of the Adhesion Society and was inducted into Phi Lamda Upsilon, a national chemistry honor society. Les obtained the M.S. degree in chemistry in January, 1990.

*Leslie Horning*